ANALYSIS OF PERIPHERAL IMMUNE RESPONSES FOR THE DEVELOPMENT OF AN ENCEPHALITIS NON-HUMAN PRIMATE ANIMAL MODEL FOR NEW WORLD ALPHAVIRUSES

by

Noah Alexander Simeon Salama

BA Cellular Molecular Biology, Washington & Jefferson College, 2015

Submitted to the Graduate Faculty of

the Department of Infectious Diseases and Microbiology

Graduate School of Public Health in partial fulfillment

of the requirements for the degree of

Master of Science

University of Pittsburgh

2017

UNIVERSITY OF PITTSBURGH

GRADUATE SCHOOL OF PUBLIC HEALTH

This thesis was presented

by

Noah Alexander Simeon Salama

It was defended on

April 19, 2017

and approved by

Thesis Director:
Amy L. Hartman, PhD, Assistant Professor, Department of Infectious Diseases and Microbiology, Graduate school of Public Health, University of Pittsburgh

Thesis Committee Members:
Simon Barratt-Boyes, BVSc, PhD, Professor, Department of Infectious Diseases and Microbiology, Graduate school of Public Health, University of Pittsburgh

William B. Klimstra, PhD, Associate Professor, Department of Immunology, School of Medicine, University of Pittsburgh

Robbie Mailliard, PhD, Assistant Professor, Department of Infectious Diseases and Microbiology, Graduate school of Public Health, University of Pittsburgh

Amy L. Hartman, PhD

ANALYSIS OF PERIPHERAL IMMUNE RESPONSES FOR THE DEVELOPMENT OF AN ENCEPHALITIS NON-HUMAN PRIMATE ANIMAL MODEL FOR NEW WORLD ALPHAVIRUSES

Noah Salama, MS

University of Pittsburgh, 2017

ABSTRACT

The New World alphaviruses eastern equine encephalitis virus (EEEV), Venezuelan equine encephalitis virus (VEEV), and western equine encephalitis virus (WEEV) are all mosquito-borne pathogens originating in North and South America. All three viruses are capable of causing severe illness in animals and humans, with extreme cases leading to encephalitis. Given the lack of commercially available vaccines or treatments, and previous research into these pathogens as potential bioterrorism weapons, all three are of great significance to public health. The aim of our laboratory was to develop a cynomolgus macaque model to study the unique neuropathology of each virus when delivered via an aerosol route, the most likely delivery route for a biological attack. To assess pathogenesis, peripheral blood mononuclear cells (PBMCs) were isolated from whole blood and analyzed by flow cytometry. Inflammation in the central nervous system (CNS) was also evaluated using a LEGENDplex bead based immunological array. Results indicate a substantial increase in the number of CCR2+ myeloid cells in circulation, a receptor important for homing and migration to infected tissue. In addition, inflammatory cytokines MCP-1 (CCL-2), IP-10, IL-6, and IL-8 were substantially upregulated in the CNS tissues and cerebrospinal fluid (CSF) of lethally infected animals. Collectively, this suggests homing and migration of peripheral immune cells to the CNS, and identifies potential markers for future longitudinal studies of alphavirus disease progression and severity.

TABLE OF CONTENTS

LIST OF TABLES

LIST OF FIGURES

ACKNOWLEDGEMENTS

To my advisor and mentor Dr. Amy Hartman. You kept me focused and driven. Your example of leadership, scholarship, and curiosity are standards that I aspire to. You have cultivated a strong and supportive environment in which young minds can broaden their research acumen and experience. I have learned more about what it means to be a scientists in the last two years working under you, than I have in a lifetime of study. You have given me the tools to move forward in my career and strive ever higher.

To my friends and lab mates Mike Kujawa, Aaron Walters, Joseph Albe, and Tiffany Thompson. We have come a long way together and shared experiences we will not soon forget. I wish all of you the best of luck in your endeavors, and thank you for your support these past two years.

To my parents, you sparked my curiosity in science and fanned the flame. I hope to continue pursuing what I love, and pass on the valuable lessons you have taught me.

1.0 INTRODUCTION

Eastern equine encephalitis virus (EEEV), western equine encephalitis virus (WEEV), and Venezuelan equine encephalitis virus (VEEV) are all members of the genus alphavirus, within group IV of the family *Togaviridae*. These three viruses are collectively called the New World alphaviruses because of their geographic distribution across North and South America. They evolved separately from another existing group known as the Old World alphaviruses, which include Sindbis and Semliki Forest virus. Although Old World alphaviruses are known to cause arthritogenic disease, the New World alphaviruses are characterized by encephalitic disease. As alphaviruses, EEEV, WEEV, and VEEV possess single-stranded positive sense RNA genomes, which contains two separate open reading frames for structural and non-structural genes. The alphavirus virion is composed of an icosahedral nucleocapsid with a monomer envelope, studded with membrane-anchored glycoproteins (E1, E2) for cell attachment and entry (1).

The US Department of Agriculture (USDA) classifies both EEEV and VEEV as Select Agents. Although WEEV is not considered a Select Agent, as a recombinant of EEEV and a Sindbis-like virus, it has major implications regarding alphavirus recombination. During the Cold War, EEEV, WEEV, and VEEV were studied by the United States and Russia as potential incapacitating agents (2). As the name suggests, all three viruses cause severe neurological pathology in equine species such as horses, donkeys, and zebras. These alphaviruses rotate

through a classical arboviral transmission cycle in which various vertebrate hosts such as birds, rodents, equids, and non-human primates serve as reservoirs (3). Outbreaks can occur in human populations and are typically preceded by a substantial outbreak in nearby equine populations, leading to medically and economically impactful disease. Regionally, these viruses are found in North and South America, although each has different zoonotic potential, given differences in vector and reservoir species (4). Mortality for most of these alphaviruses is low (4%-5%), with only a small number of naturally exposed individuals developing symptoms (5). However, symptomatic infection can rapidly progress to encephalitis with mortality rates varying for each virus: ~10% for WEEV, 30-70% for EEEV, and <1% for VEEV. Of the survivors of WEEV or EEEV encephalitis, roughly a third experience persistent neurological damage (5). No treatment or vaccine exist that are approved by the US Food and Drug Administration (FDA) for any of these viruses, and infection with one alphaviruses does not confer cross-reactive immune responses. Understanding the unique pathology of each of these viruses and the means of neuroinvasion is essential to generating viable biological interventions, and could help further elucidate neuroinvasive mechanisms of other arboviruses.

1.1 EASTERN EQUINE ENCEPHALITIS VIRUS

1.1.1 Epidemiology

Eastern equine encephalitis virus is separated into 4 distinct genetic lineages each associated with specific regions of North or South America. Lineage I is considered the North American strain, and ranges across the east and gulf states of the United States. Lineage II, III,

and IV are South American variants including those from the countries of Brazil, Venezuela, Peru, Columbia, and Argentina. The second lineage is thought to spread as far north as Central America (6). Although the geographic distribution of EEEV in North America was thought to be limited by colder weather conditions up north, in recent years cases have occurred as far north as eastern Canada (7). It was first identified as a potential human disease in 1938, when an outbreak in equine populations resulted in a subsequent outbreak across eastern Massachusetts (8). Although the infection rate in human and equine populations was low, the lethality of the virus was high. In horses, it is estimated that the mortality rate of the virus was 90%, and in symptomatic humans, it ranges from 30-70% (8, 9). According to the centers for disease control (CDC), on average there are roughly 6 human cases of EEEV in the US per year, but over the past decade there has been a resurgence of EEEV cases and an expansion of the range of the virus as far north as Nova Scotia and Canada (7).

EEEV, like WEEV and VEEV, is transmitted through a classical arboviral transmission pathway. The primary reservoir for EEEV is thought to be passerine birds, with rodents and other small mammals playing minor roles. The enzootic cycle of EEEV is maintained in freshwater fowl, typically in swamps or marshlands. The vector primarily responsible for circulation within the enzootic cycle is the *Culiseta melanura,* which feeds almost exclusively on avian species. As such, in order for an epizootic outbreak to occur a bridge vector is required to transmit to humans or other mammals. Some mosquitoes that may facilitate this bridging of enzootic to epizootic cycles include *Aedes, Coquillettidia,* and *Culex* species (10). As with most arboviruses, outbreaks of EEEV occur in a seasonal fashion in direct relation to temperature and rainfall. Humans and equines are considered dead-end hosts due to insufficient virus titers in

blood for subsequent infection of blood feeding mosquitoes, and will be discussed at greater length in the section on EEEV pathogenesis.

The major divide in classification between North American and South American strains of EEEV is based on antigenic properties. Infection or vaccination with one strain does not convey a cross-reactive immune response. Despite being an RNA virus, with expected high rates of mutation, EEEV is surprisingly conserved across samples (11). In comparison, the South American strain seems to have a more controlled rate of mutation, but is not commonly associated with human disease (12, 13). The North American strain may undergo periodic extinction events of viral strains or mutations due to low virus populations in regions with overwintering (12). Another distinction of the North American strain is in the enzootic cycle vector and host ecology. Instead of avian or mammalian reservoirs, North American EEEV may also utilize reptilian or amphibian hosts. These conditions could explain the genetic drift evolution of North American EEEV and the episodic increases in virulence.

1.1.2 Pathogenesis

EEEV, WEEV, and VEEV were originally thought to follow a similar pathogenesis due to similarities in viral life cycle, neurotropism, and genetic relationship. However, closer investigation into the pathogenesis of each virus has highlighted unique differences between New World alphaviruses. EEEV is unique in that there are little to no prodromal symptoms, meaning infected individuals exhibit no initial symptoms prior to the development of a full fever. Once symptoms have occurred, the virus has already invaded the central nervous system. Infected individuals typically experience non-differentiable acute febrile illness with chills, myalgia, arthralgia, retro-ocular pain, headache, and even loss of consciousness. From there it

rapidly progresses to more severe neurological disease, resulting in paralysis, seizures, coma, and death (14). As stated previously, mortality for symptomatic EEEV infections can range from 30%-70%. Of the survivors, roughly one third develop long-term neurological sequelae.

Klimstra and colleagues have suggested that, unlike VEEV or WEEV, EEEV is incapable of infecting most lymphoid origin cells or myeloid cells (15). The inability of EEEV to infect these cells types is controlled at the genetic level, rather than by cell adhesion and entry factors (15). Interestingly, avoidance of these tissues may reduce the production of INF-α/β *in vivo*, representing a unique evasion of host immune responses. Due to altered tropism during peripheral replication, EEEV does not exhibit the characteristic prodromal symptoms of most arboviruses. Peripheral replication seeds a viremia that reaches titers equivalent with other alphaviruses, but of shorter duration. Due to the high neurotropism of EEEV, this is sufficient for invasion of central nervous tissue and progression of encephalitis. Once in the CNS, EEEV replicates and neurological symptoms progress rapidly. While the exact mechanism of neuroinvasion remains unclear, data suggests that the virus is crossing the blood brain barrier via passive transfer (16).

Like many neurotropic arboviruses, all three New World alphaviruses are particularly virulent in adolescent populations. It is theorized that immature neurons do not have sufficient expression of neuroprotective genes such as bcl-2, which inhibit caspase dependent apoptosis (17, 18). Neuron maturity has also been shown *in vitro* to alter efficiency of viral protein synthesis and packaging (19). Alphaviruses typically halt expression of host proteins and rapidly kill infected cells. Mature neurons appear to recover host protein synthesis after infection, whereas immature neurons do not. As is often the case with lethal viral encephalitis, death is the

result of inflammation in the brain causing pressure on the brain stem, thereby stopping vital life functions.

1.2 VENEZUELAN EQUINE ENCEPHALITIS VIRUS

1.2.1 Epidemiology

VEEV was first discovered in Venezuela in 1938 (20). The virus was known to cause mild to severe disease in equine species, but no known human cases had occurred. Several years later in 1943, human cases began presenting from laboratories where VEEV isolates were being tested (21). It is believed that these cases were caused by aerosolization of virus during isolation, and VEEV has since been shown to be highly infectious by the aerosol route (22). Unfortunately, due to the geographic distribution throughout South and Central America, the presence of symptomatically indistinguishable diseases such as dengue fever, and the relative scarcity of specialized laboratory equipment for VEEV detection, disease burden remains largely unknown (23).

VEEV strains are broken down by subtype (I-VI) with subtype I further broken down into variants AB, C, D, and E. Epizootic strains include IAB and IC and enzootic strains, which cause illness in humans but not equines, include ID, IE, and IIIA (20). The life cycle of VEEV follows a classical arboviral transmission cycle with an enzootic and epizootic cycle. The enzootic cycle involves the cyclical transmission within reservoir (sylvatic) rodents, bats, birds, and equines (24). Transmission is primarily by mosquitoes with varying efficiency between species. At least 10 species are considered probable vectors within North and South America including *Aedes,*

Culex, Psorophora, Mansonia, and *Deinocerites* species. Due to the low fidelity of RNA viruses, rapid mutation in genome can cause a sudden change of phenotype and expand host range. Specifically, repeated rounds of transmission within the enzootic cycle resulting in a mutation of the E2 glycoprotein, the primary cell attachment factor, has been shown to initiate epizootic outbreaks (25). Spillover from enzootic cycles can also occur during seasons of heavy rainfall, which causes an increase in populations of vector species. Human cases usually occur in individuals who work with equine or equid species during an epizootic outbreak.

The first confirmed naturally acquired human case of VEEV was in Colombia in 1952, and the first confirmed naturally acquired case in the United States was 1968 (20). Outbreaks of VEEV have occurred sporadically from 1930-1970 throughout South America and into the southern United States. Major epizootic periods include Guajira Peninsula (1938-1942), Venezuela (1962), and Colombia (1967-1972) (26).The period from 1967-1972 caused as many as 100,000 equine deaths, and the infection of between 250,000 and 500,000 people (26). Although mortality rates for the virus remained low, the economic impact was substantial. After this period in the early 1970s, outbreaks of VEEV became rarer and it was believed that the virus was under control. Since then VEEV has re-emerged, causing outbreaks in Venezuela (1995) and Southern Mexico (1993-1996) (27-29). Adaptation to either reservoir species or vector, through variations in binding via the E2 glycoprotein, has been implied as a major determinant in the emergence of VEEV after a considerable period of inactivity (30).

1.2.2 Pathogenesis

Alphavirus infections in humans are typically asymptomatic; however, symptomatic infections can progress rapidly to lethal encephalitis. Of the three, VEEV is the least lethal, with

a mortality rate below 1% (31). The pathogenesis of VEEV demonstrates a biphasic illness starting with peripheral infection/replication, eventually leading to invasion of the CNS. In natural infections, replication begins at the site of inoculation and spreads quickly to the draining lymph node. Unlike EEEV, VEEV exhibits a strong tropism for dendritic cells, macrophages, and cells of lymphoid origin (15, 32). Although capable of infecting mesenchymal cells like EEEV, the primary site of replication appears to be dendritic cells originating in the skin, called Langerhans cells (32). These infected dendritic cells migrate to the draining lymph where the virus replicates rapidly, seeding viremia. This first phase is characterized by a non-descript febrile illness, similar to many arboviral infections. Viremia reaches relatively high titers compared to EEEV or WEEV and disseminates systemically, causing infection of peripheral lymphoid tissues. High viremia develops early in infection, but is rapidly cleared by the immune system. The brief viremia is sufficient for the invasion of central nervous tissue via the trigeminal and olfactory nerves, thereby progressing to the second phase of the disease (33). Although infection of the CNS in humans is rarely lethal, it is highly debilitating. Common symptoms include fever, headache, myalgia, arthralgia, retro-ocular pain, and chills (34). Unlike WEEV or EEEV, VEEV is not known to cause long-term neurological sequelae and even encephalitic infections have a high survival rate.

1.3 WESTERN EQUINE ENCEPHALITIS VIRUS

1.3.1 Epidemiology

Western Equine Encephalitis Virus was first identified in the 1930 as the cause of several outbreaks in equine populations throughout the western United States. Several years later in 1935, WEEV was isolated from human patients in Saskatchewan Canada (35). From1930-1950, sporadic outbreaks occurred across these regions often proceeded by nearby outbreaks in equine species by several weeks (35). Like EEEV and VEEV, WEEV follows a classical arboviral transmission cycle with passerine birds as the primary reservoir. The primary vector species for WEEV transmission is the mosquito *Culex tarsalis,* from which the virus has been isolated as early as the 1940s (36). As with most arboviral infection, a temporal relationship exists between abundance of vector species and WEEV transmission, resulting in most infections occurring during the summer (37).

Interestingly, since the initial period of WEEV activity, from 1930-1950, there has been a dramatic reduction in the number of cases each decade since (38). No additional cases have been reported in the US or Canada since 1998 (39). The cause of this rapid decline in infectivity is unclear although theories regarding environmental changes or mutations have been suggested. Given the low apparent mutation rate of alphaviruses, and recent experiments in animal models, changes in virulence does not appear to explain this trend (40). What makes WEEV unique compared to the other New World alphaviruses, is its origin as a recombinant virus. While the sequence of WEEV's capsid protein and 3' UTR region appear to have come from EEEV, the E1 and E2 glycoproteins, responsible for cell adhesion and entry, appear to have close genetic similarity to the Old World Sindbis virus (41). Through recombination, WEEV exhibits the

cellular tropism of Old World Sindbis-like viruses, but retains some of EEEV's encephalogenic properties. Although it has the potential for long-term neurological sequelae like EEEV, WEEV is substantially less lethal, with a mortality rate of less than 5% of symptomatic individuals.

Like EEEV, WEEV can cause long-term neurological sequelae, and, due to neuronal maturation, adolescents and infants appear more susceptible to infection. In addition to infants and adolescents being susceptible populations, elderly populations are also more prone to symptomatic WEEV infection. While cases have declined, WEEV remains a reportable illness with the potential to cause further epidemics. Considering its origin as a recombinant alphavirus, it also suggests possible routes of evolution for RNA viruses that could cause sudden shifts in infectivity or susceptibility.

1.3.2 Pathogenesis

WEEV infections, like other New World alphaviruses, are often asymptomatic. Those who do experience illness typically present with mild flu-like symptoms: fever, myalgia, headache, lethargy, and stiff neck. Despite close genetic relationship to EEEV, WEEV does present prodromal symptoms, which is likely due to the altered E1 and E2 glycoproteins causing differences in peripheral infection. After prodromal symptoms, WEEV can progress to encephalitic disease, with higher frequency in children and elderly populations. WEEV encephalitis often presents with headache, vomiting, neck stiffness, altered mental state, and seizures.

Neural invasion has been seen regardless of route of exposure, although the exact method of entry remains unclear. In addition, the olfactory bulb has been identified as a possible entry point, given higher viral titer in this region compared to the rest of the brain (42). WEEV

presents a hybrid-like pathology of EEEV and VEEV. Like VEEV it infects a number of peripheral cells and stimulates an adaptive response, but is also capable of developing lethal encephalitis similar to EEEV infection. It is unclear if the mechanism of neural invasion for WEEV is more like EEEV or VEEV, but given substantial difference in E1 and E2 glycoproteins it could present a novel mechanism entirely.

1.4 PUBLIC HEALTH SIGNIFICANT

1.4.1 History of New World Alphaviruses and Biological Warfare

The New World Alphaviruses EEEV, VEEV, and WEEV pose significant threats to human and equine populations as naturally occurring infections, as well as potential bioterrorism agents. There are currently no therapeutics or interventions for New World alphavirus infection approved by the US food and drug administration. All three pathogens are classified as Category B agents by the Centers for Disease Control and Prevention (43). Although WEEV has reduced dramatically in frequency over the last 3 decades, as a multi-host pathogen, WEEV, EEEV, and VEEV all have the potential for recombination events significantly altering virulence and infectivity. In addition, climate change has caused dramatic changes in arthropod geographic distribution, life cycles, and abundance. These changes in vector species have already altered viral evolution and virulence for several mosquito-borne pathogens around the world, resulting in wide spread epidemics (44).

VEEV was investigated during the period of operation of the United States Biological Warfare and Biological Defense Programs from 1942-1969 (45, 46). US biological weapons

development was halted in 1969 after two national security memoranda. Later in 1970, an international accord would be presented for the Convention on the Prohibition of the Development, Production and Stockpiling of Bacteriological (Biological) and Toxin Weapons. During this same period, the Soviet Union had a highly active bioweapons program, which designed a smallpox-VEEV chimera for aerosol transmission (2). The interest in VEEV as a biological weapons agent for both defensive and offensive application was as a debilitating agent. The bi-phasic febrile illness that is characteristic of VEEV is highly debilitating, and because it is non-lethal, there is reduced risk of collateral damage.

While VEEV was of primary investigation for offensive development, WEEV and EEEV were also research by the United States as part of a defensive biological program. All three New World alphaviruses grow to high titer in stock, making production on a large scale simple and relatively cheap (47). Even more alarming is the ease with which reverse genetic systems can be utilized to genetically alter these viruses to increase virulence (48, 49). In addition, New World alphaviruses are highly stable in aerosol form. These aspects make EEEV, VEEV, and WEEV ideal targets for biological weaponization, and therefore of high concern. Given their history of weaponization, their potential for artificially induced virulence, potential for mortality or long-term morbidity, expanding vector species range, and potential for co-infection and recombination with other arboviral species, further investigation into New World alphaviruses is essential to global health and security.

2.0 STATEMENT OF PROJECT AND SPECIFIC AIMS

Neurological disease caused by the New World alphaviruses Eastern, Western, and Venezuelan Equine Encephalitis virus is poorly understood. In studying especially lethal or disabling pathogens that affect humans, it is necessary to establish models that can be used to mimic human disease as closely as possible. In the case of encephalitic alphaviruses, in order test vaccines, anti-virals, or other interventions, it is necessary to apply the FDA Animal Efficacy Rule or Animal Rule (50). This rule is applied to the development of biological interventions for life-threatening diseases when human efficacy trials are either infeasible or unethical. For this study, we built upon previous work that established cynomolgus macaques as a potential model for New World alphaviruses EEEV, WEEV, and VEEV. The overarching goal of the larger project is to identify biomarker(s) of impending viral encephalitis or disease severity in all 3 viruses. As a first step towards this goal, we characterized the peripheral immune responses in cynomolgus macaques as a result of aerosol exposure to EEEV, WEEV, and VEEV. Our hypothesis is that there will be measurable changes in peripheral blood immune cell populations, blood chemistry parameters, and/or inflammatory cytokines that will correlate with the onset of viral encephalitis (for EEEV and WEEV) or acute febrile illness (for VEEV) as well as an indication of disease severity. These data, in combination with telemetry, CT-scans, and neurological symptoms, could be useful for identifying important clinical windows for intervention.

2.1 AIM 1: IDENTIFY CHANGE IN PERIPHERAL BLOOD LYMPHOID AND MYELOID POPULATIONS IN CYNOMOLGUS MACAQUES INFECTED WITH EEEV, VEEV, AND WEEV

Based on previous models of alphavirus infection by aerosol route in cynomolgus macaques, we expect lymphopenia and granulocytosis in peripheral immune cell populations; however, further delineation of changes in cell populations has not been done.

We hypothesize that, due to the importance of T cells for clearance of viral infection of the CNS (51), there will be a direct correlation between increased disease severity in the lethally-infected animals and decreases in overall T cell numbers. We also predict that given the rapid progression of lethal EEEV infection (5-6 days), the innate immune system may play an important role in survival. To address this aim, comparisons will be made between pre- and necropsy (PRE vs NEC for lethally infected animals), pre-infection and convalescence in survivors (PRE vs CONV in survivors). By comparing PRE/NEC and PRE/CONV samples within each virus as well as between all 3 viruses, we will determine if there are major changes in cell populations over the course of infection.

To address this aim, we will perform the following assays:

1. Complete blood count (CBC) and blood chemistry analysis on blood samples from each animal at each time point.

2. Isolate peripheral blood mononuclear cells (PBMCs) from whole blood prior to infection and at the time of necropsy. The flow cytometry staining protocol will be optimized in order to easily identify various lymphoid and myeloid cell populations using flow cytometry [T cells, NK cells, B cells, plasmacytoid dendritic cells (pDCs), myeloid dendritic cells (mDCs), brain homing macrophages, classical, non-classical, and

intermediate monocytes]. Cell numbers will be normalized to complete blood count (CBC) parameters and against expression of pan-leukocyte marker CD45. In addition to identification quantification of cell types, we will assess differences in activation marker expression (HLA-DR) (potential future activation markers CD81, intracellular markers Ki-67, or pro-inflammatory cytokine production).

2.2 AIM 2: IDENTIFY PERIPHERAL INFLAMMATORY BIOMARKERS ASSOCIATED WITH LETHAL VS SUBLETHAL DISEASE IN THE PLASMA AND CSF, AND CORRELATE THESE FINDINGS WITH BRAIN TISSUE

As with Aim 1, comparisons will be made between PRE/NEC and PRE/CONV samples from the same animal, as well as across animals infected with each of the viruses. We hypothesize that cytokines that are dysregulated in the brain tissues itself are also detectable in the serum and/or CSF. By comparing endpoint samples from necropsy to pre-infection samples, we will be able to detect changes in the periphery that correlate with what is happening in the CNS tissue. Previous work in mice suggests a hierarchy of inflammatory cytokine dysregulation in the periphery (VEEV>WEEV>EEEV) (1). Future studies will use the results found here to examine earlier (pre-necropsy) samples to identify early biomarkers of lethal encephalitis.

To address this aim, we will obtain pre-infection and post-infection serum samples, CSF (from necropsy), and homogenized brain tissues from the cerebellum, frontal cortex, parietal lobe, occipital lobe, and temporal lobe. Samples will be analyzed for cytokine and chemokine expression using BioLegend's LEGENDplex 13-parameter bead-based immunoassay. The

inflammatory markers we will measure include: IL-6, IL-10, CXCL10, IL-1 β, IL-12p40, IL-17A, IFN- β, IL-23, TNF- α, IFN- γ, GM-CSF, IL-8, and CCL2.

3.0 MATERIALS AND METHODS

3.1 BIOSAFETY

All experiments using the live virulent strains V105 of EEEV, INH9813 of VEEV, and FLEMING of WEEV were performed in the Regional Biocontainment Laboratory at the University of Pittsburgh. This facility is approved by the Division of Select Agents and Toxins (DSAT) and the USDA to work with Tier 1 Select Agents. All work was conducted in class II biosafety cabinets connected to external HEPA filters, and no air was recirculated into the lab. Every worker was required to abide by Biosafety Level 3 practices, and use powered air purifying respirators (3M Versaflo TR-300 PAPR unit) within containment labs. All animal work was performed under Animal Biosafety Level 3 practices, and operated under strict institutional animal care and use committee (IACUC) approval. All animal work requiring sharps for EEEV or VEEV infected animals was performed by vaccinated technicians with sufficient antibody titers. For decontamination, Vesphene IIse in a 1:128 dilution was used with a minimum contact time of fifteen minutes before being marked for further decontamination via autoclave.

3.2 AEROSOL

All aerosol infections were performed by Dr. Douglas Reed and his lab. Aerosol generation for each virus was performed using an Aeroneb, vibrating-mesh nebulizer. Aerosols were delivered to the animal in a head only exposure chamber via the AeroMP Exposure System, housed within a Class III biosafety cabinet. To maintain a constant breathing rate, each animal had a pump for continual anesthetic during the exposure. Plethysmography data were calibrated based on airflow changes in a chamber adjacent to the head only exposure chamber, allowing us to calculate the exact dose delivered to the animal based on loading titer, time, lung volume, and respiration rate. At this stage in the study we are attempting to identify an ID100 for each virus. The target titer to challenge the first animal was E+07, with subsequent infections of other animals being approximately 1 log above or below the first infection. Animals were necropsied when they met necropsy criteria or after convalescence (28 days post exposure). Animals were monitored by telemetry implants for ECG, EEG, and temperature, and 24/7 video surveillance prior to exposure, and until necropsy or until observations scored the animal at a 3 for one week.

3.3 BLOOD DRAWS AND CELL ISOLATION

Baseline blood samples were taken from all monkeys at the housing facility in Plum. Blood was collected in ethylenediaminetetraacetic acid (EDTA) vacutainers (purple top), sodium heparin vacutainers (green top), and plain vacutainers (red top). Blood treated with sodium heparin was used for blood chemistry analysis on a Vetscan VS2 Abaxis blood chemistry machine. CBC data was collected from EDTA treated blood run on a Vetscan HM2 Abaxis

Hematology Analyzer. Blood in plain vacutainers and EDTA vacutainers was centrifuged at 2500rpm for 10 minutes at room temperature (RT), no brake. Plasma and serum were collected off of each tube and stored in aliquots of either 500uL or 1mL depending on the amount of blood being processed.

The remaining blood in each EDTA vacutainer was transferred to 50mL conical tubes (no more than 15mL blood per tube) for isolation of peripheral blood mononuclear cells (PBMC). Sterile RT Dulbecco's phosphate-buffered saline (DPBS) quantum satis (QS) was added, total volume of 35mL. Once the blood was diluted, lymphocyte separation medium (LSM) was used to create a density gradient to separate mononuclear cells. For each 50mL conical of blood, 13mL of LSM was applied as an underlay and each tube was then centrifuged at 2000rpm for 25 minutes at RT, 3 acceleration no brake. After spinning, the buffy coat layer was extracted by manual pipette and transferred to fresh 50mL conical tubes. The isolated cells were washed with sterile RT DPBS (QS), 50mL total volume. Cells were pelleted by spinning at 1800rpm for 10 minutes at 4˚C. The supernatant was removed and cells were resuspended by flicking. To lyse red blood cells 10mL of ammonium-chloride-potassium (ACK) lysis buffer was added to each tube and they were incubated at RT for 10 minutes. After red blooc cell (RBC) lysis, cells were washed with 40mL of RT DPBS and spun at 1800rpm for 10 minutes at 4˚C. The supernatant was discarded and cells were resuspended with 30mL of 4˚C DPBS. Then we did a slow cold spin to remove platelet contamination (1200rpm, 15 minutes, 4˚C, no brake). Supernatant was pulled out using a 10mL serological pipette and the pellet was resuspended by flicking. Finally we resuspended the cells to a desired concentration (3-5e^6 cells/mL target, up to 20e^6 cells/mL) using freezing media [90% fetal bovine serum (FBS), 10% dimethyl sulfoxide (DMSO)]. All centrifugation done using Sorvall Legend RT benchtop centrifuge.

3.4 SPLEEN CELL ISOLATION

During necropsy 0.3 grams of spleen was removed and transferred to a 50mL conical fill with Hanks buffered salt solution (HBSS) w/o calcium and magnesium. Spleen sample was transferred to LS3 for further processing and cell isolation. Spleen tissue was removed from 50mL conical and incubated for ~1 hour at RT with a digestion (1mg/mL collagenase 1-A, and 50µg/mL DNAse 1, in HBSS w/ Ca/Mg). Once tissue was soft enough to manual digestion, it was cut into smaller pieces and placed in a 15mL conical with (QS) of digestion buffer, max volume 7.5mL. The chopped tissue was then place on a rocker in an incubator at 37˚C (45-60 minutes). After incubating, the tissue was further broken down using a 5mL serological pipette until it flowed smoothly. After the serological pipette, a manual transfer pipette was used to vigorously pipette up and down until it flowed smoothly. The further homogenized tissue was placed back on the rocker to incubate at 37˚C for 30-45 minutes. After incubation, the tubes were removed and cells passed through a small transfer pipette to clear any visible chunks. Next, the homogenized tissue was added to a fresh 50mL conical after being passed through a 40µm cell strainer. Any homogenized material that did not go through the filter was taken off the top and added directly to the 50mL conical, leaving behind large chunks caught in the cell strainer. The cell strainer was washed with 12mL of wash buffer consisting of 50µg/mL DNase 1 in HBSS w/o Ca/Mg with 3% FBS. Then cells were spun at 500g for 8 minutes at RT. Supernatant was removed and the cells were washed again with 18mL of wash buffer and spun at 500g for 8 minutes at RT. The supernatant was removed and the pellet resuspended with 10mL of 80% stock isotonic percoll (SIP) solution and transferred to a fresh 50mL conical. Then we overlayed the cells with SIP layers at decreasing concentrations to form a density gradient: 10mL of 38% SIP, 10mL 21% SIP, and 5mL of HBSS/3% FBS. The sample was then spun at 480g for 35

minutes at 18˚C, acceleration 3 no brake. After the spin, the top two interphases were discarded and the fraction at the 3rd interphase was placed in a new 50mL conical tube. The extracted cells were washed with 30mL of HBSS w/o Ca/Mg w/ 3% FBS and centrifuged at 300g for 8 minutes, RT. The pelleted cells were resuspended by flicking and incubated at RT with 10mL of ACK lysis buffer for 10 minutes, swirling occasionally. After red blood cell lysis, the cells were washed again with 40mL of RT DPBS and spun at 1800rpm for 10 minutes at 4˚C to pellet the cells. The cells were resuspended in freezing media [90% FBS, 10% DMSO] and put in 1mL aliquots for long-term storage in liquid nitrogen after step-down freezing.

3.5 STAINING AND FLOW CYTOMETRY

Cells were either stained fresh from isolation or from cryopreserved cells stored after necropsy. Every stain used from 1-1.5 million cells per well. For fresh stains, cells resuspended in FACS buffer were added in 250µL increments to a 96-well V-bottom plate until desire cell concentration was reached. Frozen cells (1mL) were thawed, and diluted in 9mL of fluorescence –activated cell sorting (FACS) buffer [1XDPBS, 3% FBS, 5mM EDTA, 0.1% sodium azide] in order to wash off DMSO. Samples were then spun with a Sorvall Legend RT bench centrifuge at 1800rpm, for 10 minutes at 4˚C and the supernatant removed. The pellet was resuspended in FACS buffer to reach the desired cell concentration and added to a 96-well V-bottom plate. The plate was spun at 1800rpm using a microplate swinging bucket rotor in a Rotanta 460r benchtop centrifuge for 5 minutes at 4˚C. Supernatant was removed by quickly inverting the plate, and cells were resuspended with 20µL of an antibody master-mix specific to each panel, as shown in

Tables 1-2. All antibodies were purchased from BD Bioscience with the exception of NKG2A (clone Z199), which is from Beckman Coulter.

Table 1. Flow Cytometry Lymphocyte Panel

Antibodies	Clone	Volume (µL)
CD3-PacBlue	SP34-2	2
CD4-PE	M-T477	2
CD8-PE-Cy7	SK1	2
HLA-DR-PerCP-Cy5.5	L243	2
CD20-APC-H7	2H7	2
CD45-FITC	D058-1283	2
CD16-V500	3G8	2
NKG2A-APC (iso)	Z199	2
FACS Buffer		4
		Total Volume 20

Table 2. Flow Cytometry Myeloid Panel

Antibodies	Clone	Volume (µL)
CD3-APC-Cy7	SP34-2	2
HLA-DR-PerCP-Cy5.5	L243	2
CD20-APC-H7	2H7	2
CD45-FITC	D058-1283	2
CD123-PE-Cy7 (leave out)	7G3	2.5
CD1c-PE (iso)	L161	2.5
CD16-BV421	3G8	2
CD14-V500	M5E2	3
CCR2-AF647 (iso)	48607	2
		Total Volume 20

The antibody mix was pipetted up and down to thoroughly resuspend the cells. Next, the plate was incubated at 4˚C for 30 minutes. After staining, the antibody stain was diluted by adding 200µL of FACS buffer and the plate was spun at 1800rpm for 5 minutes at 4˚C. The wash was repeated again and the pellet was resuspended with 200µL of 4% PFA and transferred to a 5mL snap cap FACS tube. The tubes were left to sit overnight at 4˚C to fix cells and inactivate virus before taking samples out of containment. All samples were run on an LSRII flow cytometer and analyzed in FlowJo version 7.6.5.

3.6 BIOLEGEND LEGENDPLEX

We used a Biolegend 13-plex NHP inflammation LEGENDplex kit to analyze the levels of inflammatory cytokines in neural tissue, serum, and CSF is convalescent and lethally infected animals. Cytokines analyzed in the panel included IL-6, IL-10, CXCL10 (IP-10), IL-1β, IL-12p40, IL-17A, IFN-β, IL-23, TNF-α, IFN-γ, GM-CSF, IL-8, and CCL2 (MCP-1). Four tissue, samples of 0.2 grams each were taken from frontal lobe, temporal lobe, occipital lobe, parietal lobe, and cerebellum. These samples were stored in 1.5mL of modified DPBS [1% FBS, 100U/mL penicillin, 0.05mg/mL streptomycin]. The samples were stored at -80˚C before preparation for multiplex. The samples were fully thawed and transferred to 5mL snap cap tubes for homogenization we used a handheld electric homogenizer. The homogenized tissues were spun at 2500rpm for 10 minutes at RT. The clarified homogenate was transferred back to their original 2mL screw top tubes and samples were taken for further dilution and analysis. Convalescent animal samples were run undiluted, while animals that were lethally infected were run at a 1:2 dilution of sample to LEGENDplex assay buffer. The kit standard was prepared using 1:4 serial dilution. All kit reagents were allowed to warm to RT before use. All samples and standards were run in duplicate on a 96 well plate. Each well had 25µL of Assay Buffer, and 25µL of either standard or sample (at desired dilution). Plasma samples also had an additional 25µL of Matrix B. Mixed beads were vortexed for 1 minute before applying 25µL to each well. The plate was covered with a plate sealer and wrapped in aluminum foil, then shaken at 500rpm for 2 hours at RT. After shaking the beads were pelleted by spinning the plate at 1050rpm for 5 minutes at RT. The supernatant was removed by quickly inverting the plate and gently blotted with a paper towel. The beads were washed with 200uL of LEGENDplex washing Buffer and spun again at 1050rpm for 5 minutes at RT. The supernatant was removed and 25µL of detection

antibodies was added to each well. The plate was sealed with a fresh plate sealer, wrapped in aluminum, and shaken at 500rpm for 1 hour at RT. After shaking, 25µL of SA-PE was immediately added to each well and the plate was shaken again at 500rpm for 30 minutes at RT. The plate was spun down at 1050rpm for 5 minutes at RT and the supernatant removed by quickly inverting the plate. The beads were resuspended with 150µL of Wash Buffer and transferred to labeled 5mL snap cap FACS tubes. All samples were run on a FACSAria flow cytometer by Timothy Sturgeon and analyzed using Biolegend LEGENDplex software.

4.0 RESULTS

4.1 AIM 1: IDENTIFY CHANGE IN PERIPHERAL BLOOD LYMPHOID AND MYELOID POPULATIONS IN CYNOMOLGUS MACAQUES INFECTED WITH EEEV, VEEV, AND WEEV

To assess the changes in peripheral immune cell populations, PBMCs were isolated from whole blood collected at pre-infection and at necropsy, as described in materials and methods 3.3. These cells were stained to identify lymphoid, and myeloid lineages (Figures 1, 2). Cell count for the lymphoid stain was calculated as a percentage of the parent population (CD45 high, forward scatter low, side scatter low, minus monocyte spillover). CD45 is a commonly expressed pan-leukocyte marker, which is found in abundance on lymphocytes, monocytes, and granulocytes, but not on mature erythrocytes. Because granulocytes are pelleted during the LSM gradient separation step, they are absent from the FACS analysis. The lymphocytes are easily identified by their small size and granularity on a side scatter by forward scatter analysis. There can still be overlap with the monocyte population, which was identified as being CD3(-), CD20(-), CD8(-), HLA-DR+. These monocytes were subtracted from the total CD45(+) gate to generate the parent population. Cell count for the myeloid stain was calculated as a percentage of Gate 4 (HLA-DR+, Lineage-). HLA-DR is an MHC Class II cell surface receptor predominantly found on antigen presenting cells. B cells and T cells are also capable of expressing HLA-DR at

relatively high rates, so these cells are excluded as part of the Lineage+ positive population using CD3 (T cell marker) and CD20 (B cell marker). Only cells that are HLA-DR+, CD3-, and CD20- are considered part of the myeloid lineage, which is used as the parent population.

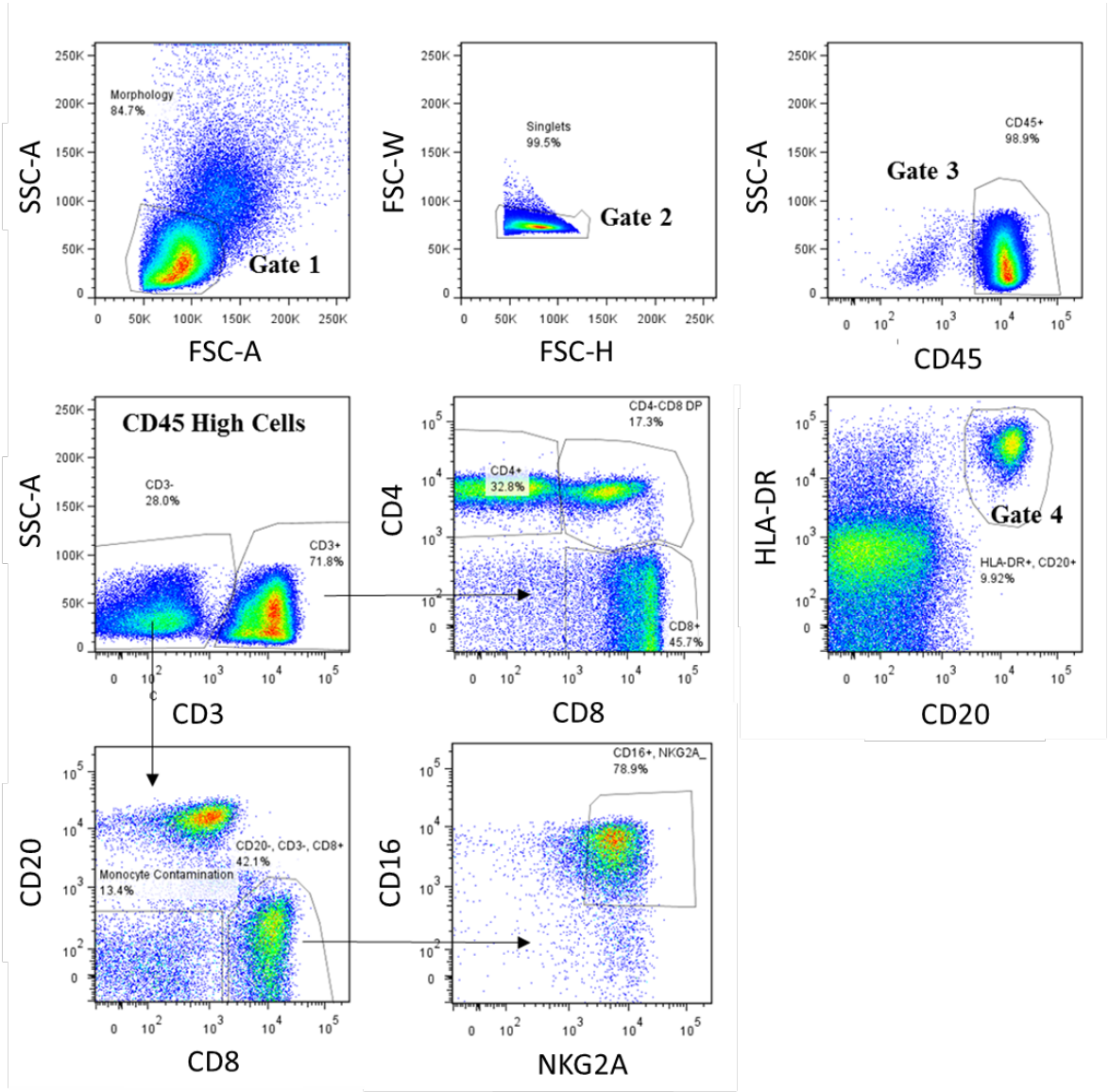

Figure 1. Gating Strategy for Lymphocyte Populations from PBMC

Gate 1 (morphology), identifies lymphocytes as a forward scatter and side scatter low population. Gate 2 (doublet exclusion), removes clumped cells from analysis, which may fluoresce in multiple channels, as being non-linear on a FSC width, by FSC height graph. Gate 3 (CD 45 high), selects for cells positive for pan-leukocyte marker CD45. Gate 4 identifies CD20 and HLA-DR double positive cells from the CD45 high expression population. CD45 high

cells were divided based on CD3 expression for further analysis. CD3- cells are further gated down to identify CD8+, CD20-, CD16(+ or -), and NKG2A(+) cells. CD3+ cells were separated based on CD4 and CD8 expression.

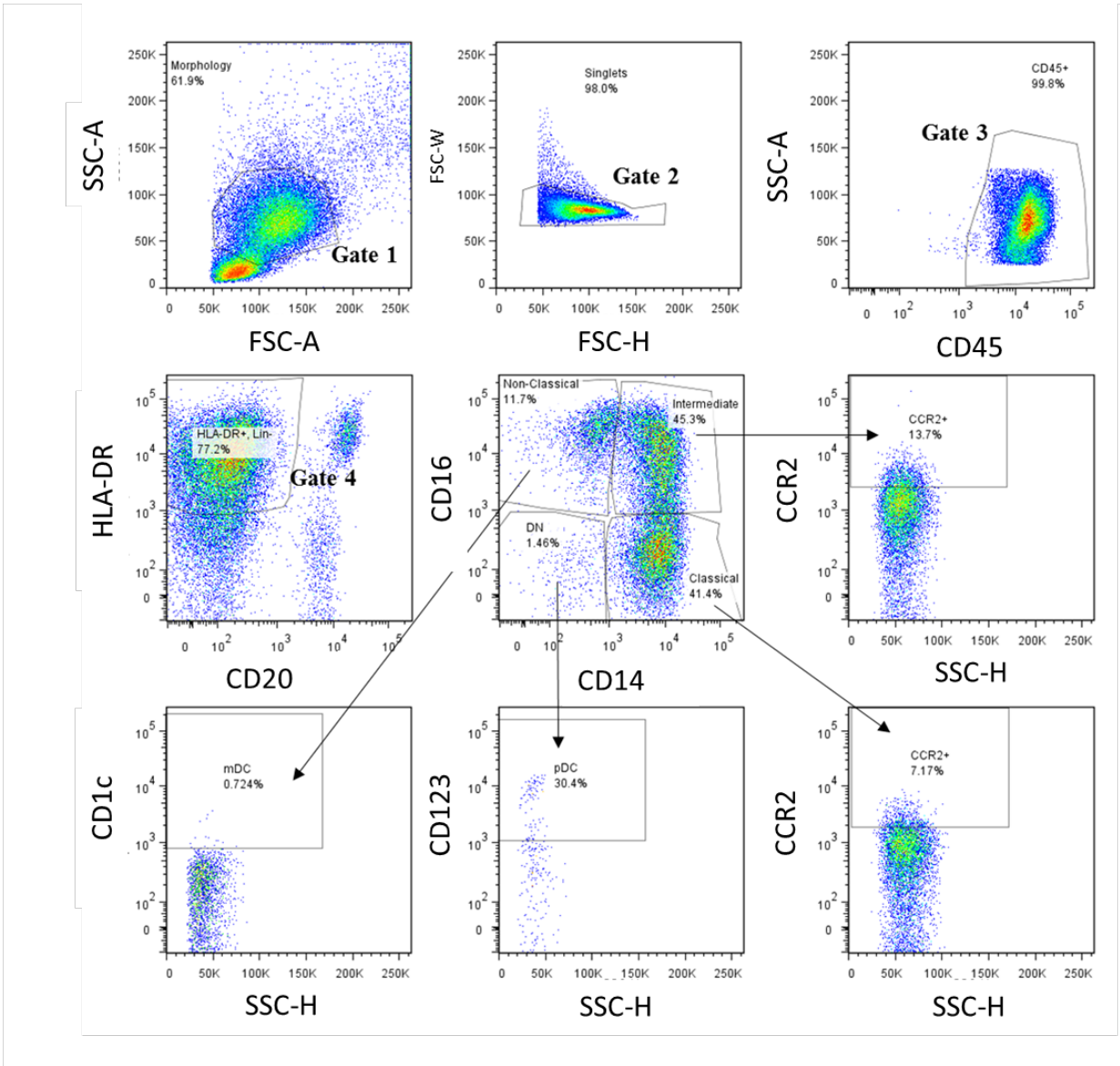

Figure 2. Gating Strategy for Myeloid Populations from PBMC

Gate 1 (morphology), identifies monocytes based on size and granularity. Gate 2 (doublet exclusion), removes clumped cell from analysis, which may fluoresce in multiple channels, as being non-linear on a FSC width, by FSC height graph (Doublets also excluded by SSC width, by SSC height, graph not shown). Gate 3 (CD45 high), selects for cells positive for pan-leukocyte marker CD45. Gate 4 identifies CD45 expressing cells that are positive for HLA-DR, but (lineage -) negative for CD3 and CD20. This population is further broken down by CD16 and CD14 to identify sub-classifications of monocytes: classical (CD14+/CD16-), non-classical (CD14-/CD16+), intermediate (CD14+/CD16+), and double negative DN (CD14-/CD16-). To identify plasmacytoid dendritic cells (pDCs), DN monocytes were analyzed for CD123 expression. Myeloid dendritic cells (mDCs) were isolated from the non-classical population as being CD1c positive. Classical and intermediate monocyte populations were also analyzed for CCR2 expression levels. Gating for mDC, pDC, and CCR2 were all based on isotype controls.

Five animals in total were challenged with EEEV by aerosol route. Of those animals, two (M161 and M163) reached sacrifice criteria by day 6 post infection, while the other three (M123, M160, M162) survived through to convalescence and were necropsied greater than 27 DPI. M160 was the first animal infected for the study and it was unclear if the animal received the desired dose during infection. As a result, it was decided to re-challenge the animal, which it also survived. M160 was eventually necropsied 19 days post secondary infection. All EEEV infections, doses, and outcomes can be found in Table 3.

Table 3. EEEV Animal, Virus, Dose, and Outcome

Animal #	Infection Date	Dose	Outcome	Necropsy
M123	1/13/17	1.50E+07	Survived	27 DPI
M160	8/26/16* 10/06/16	1.10E+07* 2.98E+08	Survived* Survived 2nd	19 DPI 2nd
M161	10/14/16	1.60E+08	Died	6 DPI
M162	10/28/16	4.64E+05	Survived	32 DPI
M163	9/02/16	3.39E+07	Died	6 DPI

EEEV

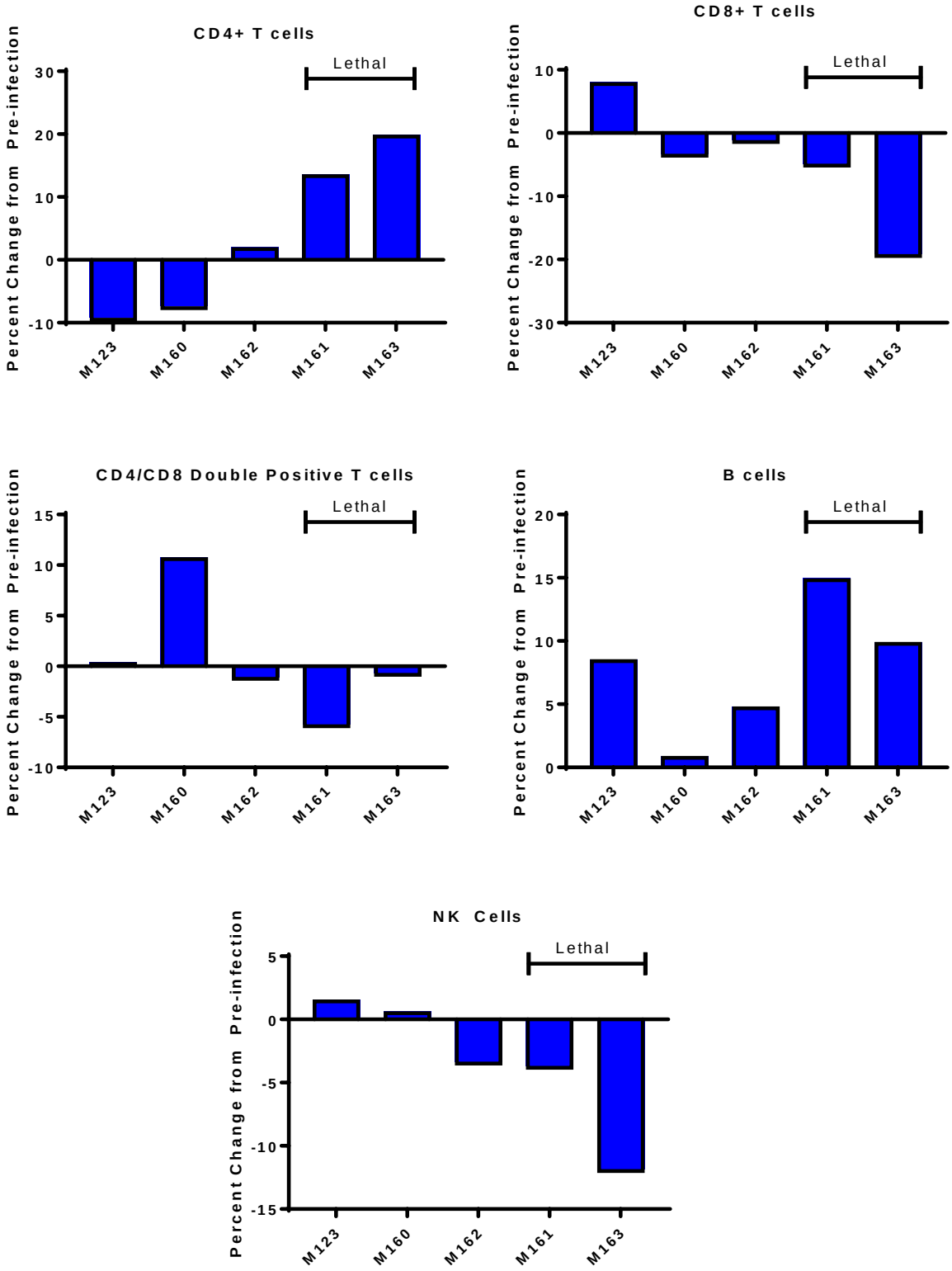
CD4+ T cells
Percent Change from Pre-infection
Lethal
30
20
10
0
-10
M123
M160
M162
M161
M163
CD8+ T cells
Percent Change from Pre-infection
Lethal
10
0
-10
-20
-30
M123
M160
M162
M161
M163
CD4/CD8 Double Positive T cells
Percent Change from Pre-infection
Lethal
15
10
5
0
-5
-10
M123
M160
M162
M161
M163
B cells
Percent Change from Pre-infection
Lethal
20
15
10
5
0
M123
M160
M162
M161
M163
NK Cells
Percent Change from Pre-infection
Lethal
5
0
-5
-10
-15
M123
M160
M162
M161
M163

Figure 3. Change in Peripheral Immune Populations, Lymphoid Lineage (EEEV).

Monkeys infected with EEEV had blood collected at pre-infection and at necropsy. PBMCs were isolated from these samples and stained to identify lymphoid lineage cells. Percentages were calculated for B cells and NK cells using CD45 high cells minus monocyte cells (CD3-, CD20-, CD8-, HLA-DR+) as the parent population. T cell population subsets were calculated as a percentage of CD3+ cells to reduce percentage fluctuation as the result of changes in other lymphoid populations.

Although insufficient animal numbers exists for robust statistical analysis, a number of trends are apparent in comparing pre-infection samples to necropsy for lethally infected animals. CD4 T cells appear to increase in number, whereas CD8 and CD4/CD8 double positive populations drop during the course of lethal infection (Figure 3). NK cell populations also appear to decrease in lethally infected animals. It is difficult to identify any definitive trends in B cell populations at this time, although serological analysis in the future may elucidate unique differences. It is impossible to rule out the likelihood that similar trends are also occurring in convalescent animals at earlier time points. Bracketing of lethal animals is purely for visual separation. Because of differences in time points of necropsy samples, lethal and convalescent samples were not statistically compared to one another for any animals or viruses.

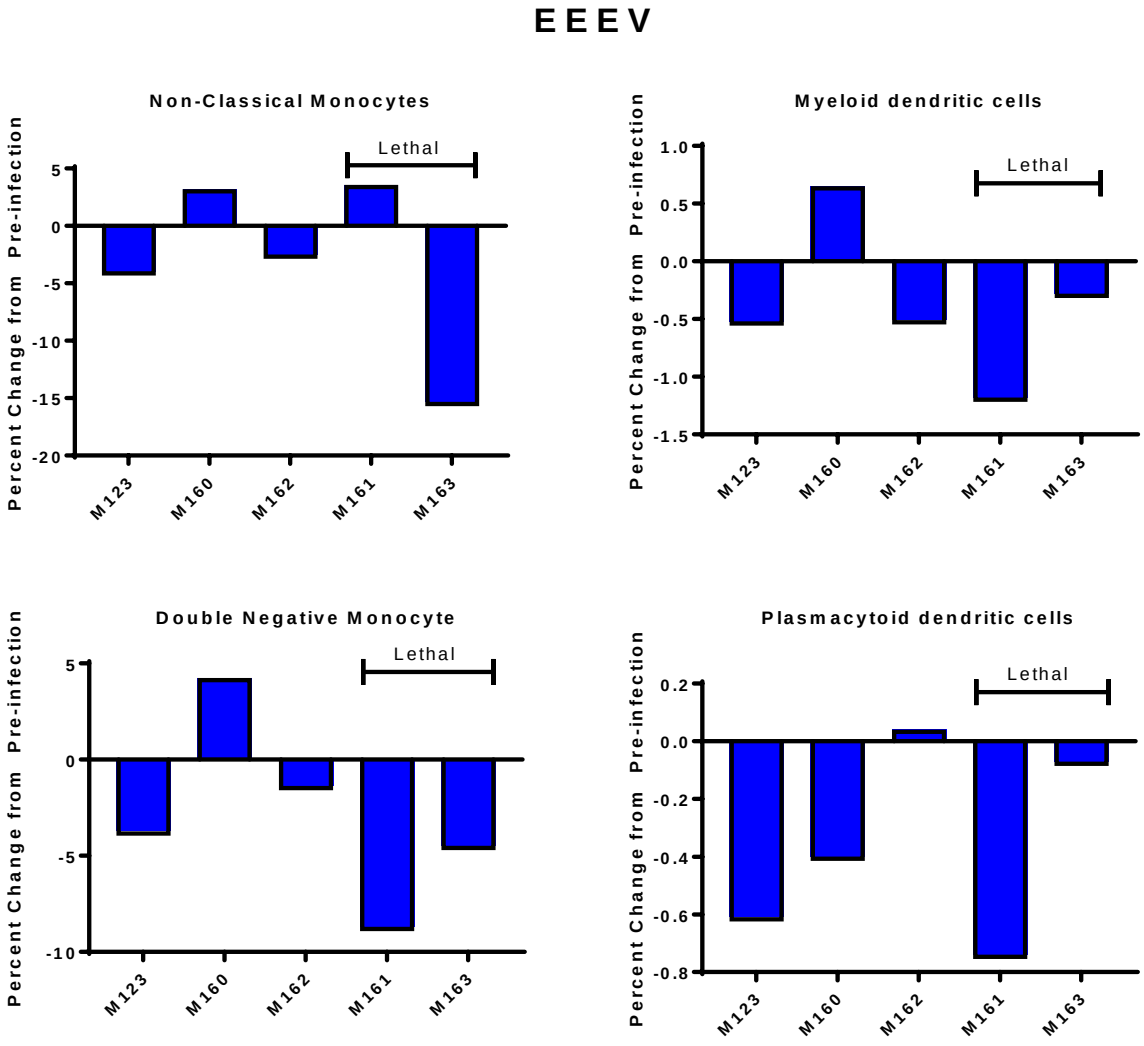

Figure 4. Change in Peripheral Immune Populations, Myeloid Lineage (EEEV)

Monkeys infected with EEEV had blood collected at pre-infection and at necropsy. PBMCs were isolated from these samples and stained to identify myeloid lineage cells. Percentages were calculated using HLA-DR+, CD3-, CD20- cells as the parent population. Difference between necropsy and pre-infection shows how progression of the disease alters peripheral immune populations.

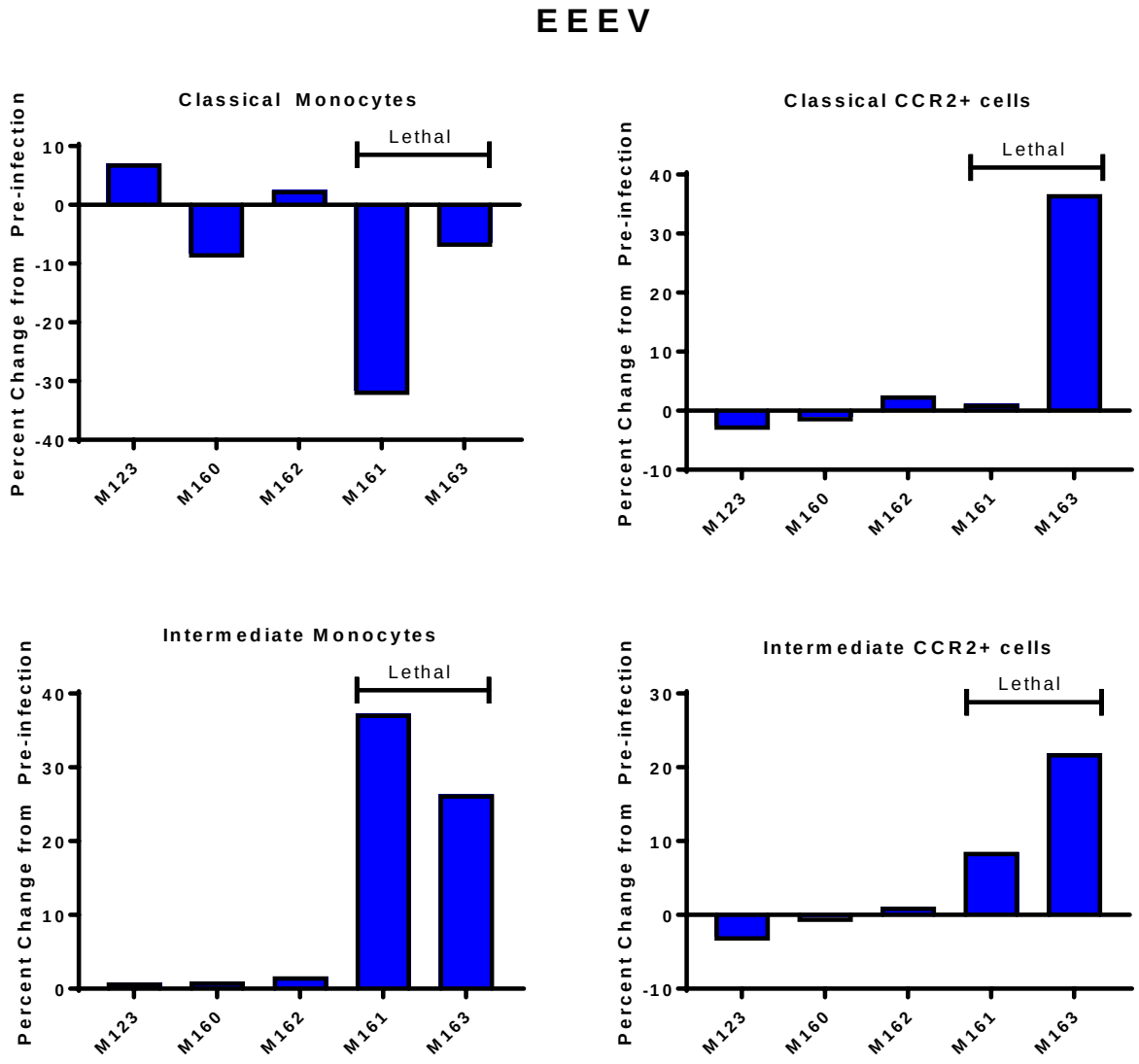

Figure 5. Change in Peripheral Immune Populations, Myeloid Lineage continued (EEEV)

Monkeys infected with EEEV had blood collected at pre-infection and at necropsy. PBMCs were isolated from these samples and stained to identify myeloid lineage cells. Percentages were calculated using HLA-DR+, CD3-, CD20- cells as the parent population. Difference between necropsy and pre-infection shows how progression of the disease alters peripheral immune populations.

These data tentatively suggests that non-classical (CD16+, CD14-) and double negative (CD16-, CD14-) monocyte populations decrease in lethally infected animals over the course of infection (Figure 4). Convalescent animals exhibit no trends in intermediate, double negative, non-classical, or classical monocyte populations when comparing pre-infection to necropsy

(Figures 4, 5). It is difficult to identify trends in more specialized populations such as mDCs and pDCs because of their relative lack of abundance compared to other leukocytes in the blood. It appears that classical (CD16-, CD14+) decrease and intermediate (CD16+, CD14+) monocyte populations increase in lethally infected animals over the course of infection (Figure 5). Furthermore, the percentage of CCR2+ cells within both of these populations is also increased during disease course (Figure 5). CCR2 is a receptor that recognizes the chemokine CCL2, which drives leukocyte homing and migration toward infected tissues. The high expression of CCR2 on these cell types indicates active migration of these cell types, although activation and migration of other leukocytes cannot be ruled out through other homing markers. Although gating and analysis are not shown, CCR2 is not upregulated in non-classical or double negative monocyte populations for lethal or convalescent animals.

Four animals have been challenged by aerosol route with VEEV so far in this study (M164, M165, M170, and M171). All four survived infection and were sacrificed at later dates (26DPI, 27DPI, 28DPI, and 29DPI respectively). The doses and outcomes can be found in Table 4.

Table 4. VEEV Animal, Virus, Dose, and Outcome

Animal #	Infection Date	Dose	Outcome	Necropsy
M164	11/04/16	1.27E+07	Survived	26 DPI
M165	11/04/16	7.88E+-6	Survived	27 DPI
M170	1/09/17	2.22E+06	Survived	28 DPI
M171	1/09/17	1.02E+06	Survived	29 DPI

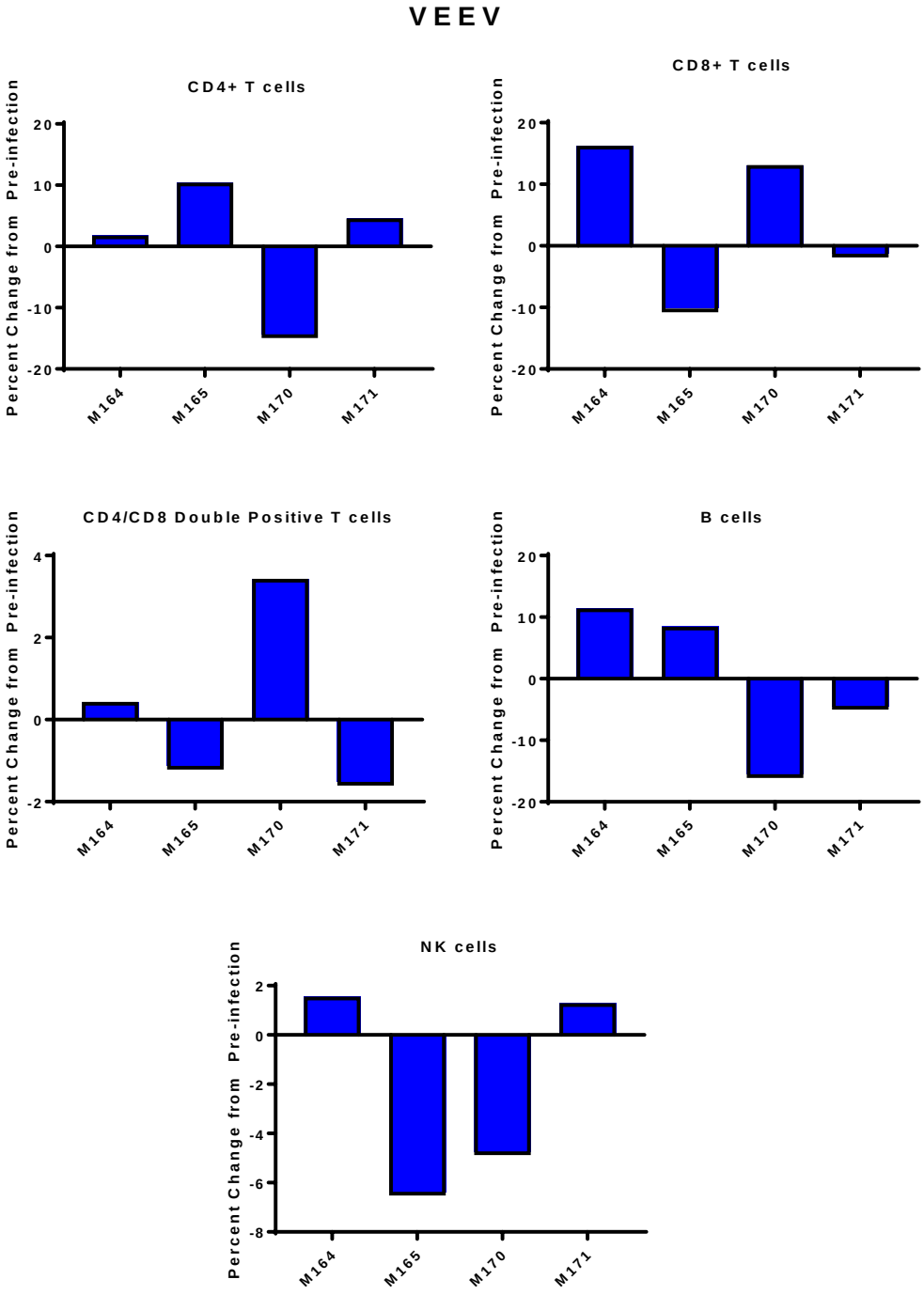

Figure 6. Change in Peripheral Immune Populations, Lymphoid Lineage (VEEV)

Monkeys infected with VEEV had blood collected at pre-infection and at necropsy. PBMCs were isolated from these samples and stained to identify lymphoid lineage cells. Percentages were calculated for B cells and NK cells using CD45 high cells minus monocyte cells (CD3-, CD20-, CD8-, HLA-DR+) as the parent population. T cell population subsets were calculated as a percentage of CD3+ cells to reduce percentage fluctuation as the result of changes in other lymphoid populations. Difference between necropsy and pre-infection shows how progression of the disease alters peripheral immune populations. No animals succumbed to infection.

It is difficult to identify trends from changes in lymphoid populations during VEEV infection without lethal infection or earlier time points. One potential trend is the reduction in NK cells when comparing convalescence with pre-infection samples (Figure 6). All animals exhibited the characteristic biphasic fever associated with VEEV infection, with varying levels of severity.

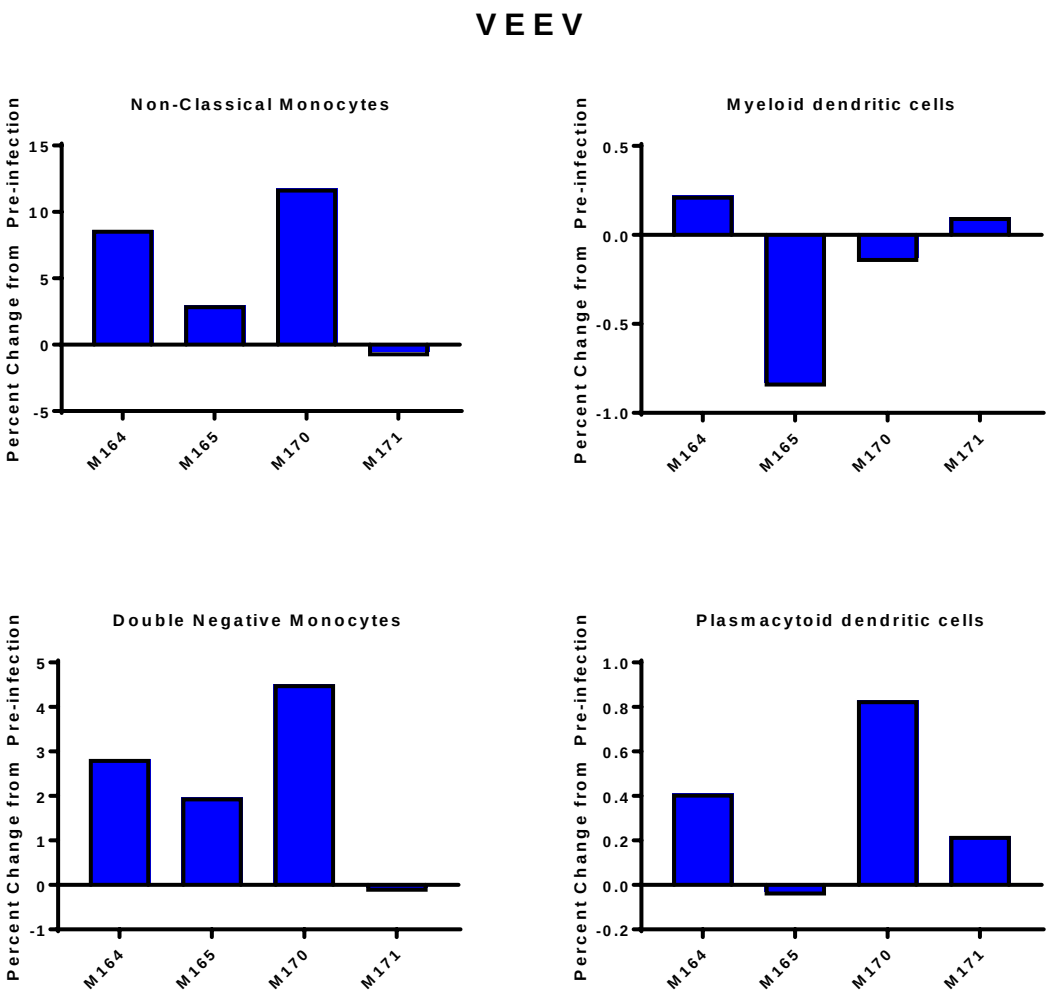

Figure 7. Change in Peripheral Immune Populations, Myeloid Lineage (VEEV)

Monkeys infected with VEEV had blood collected at pre-infection and at necropsy. PBMCs were isolated from these samples and stained to identify myeloid lineage cells. Percentages were calculated using HLA-DR+, CD3-, CD20- cells as the parent population. Difference between necropsy and pre-infection shows how progression of the disease alters peripheral immune populations. No animals succumbed to infection.

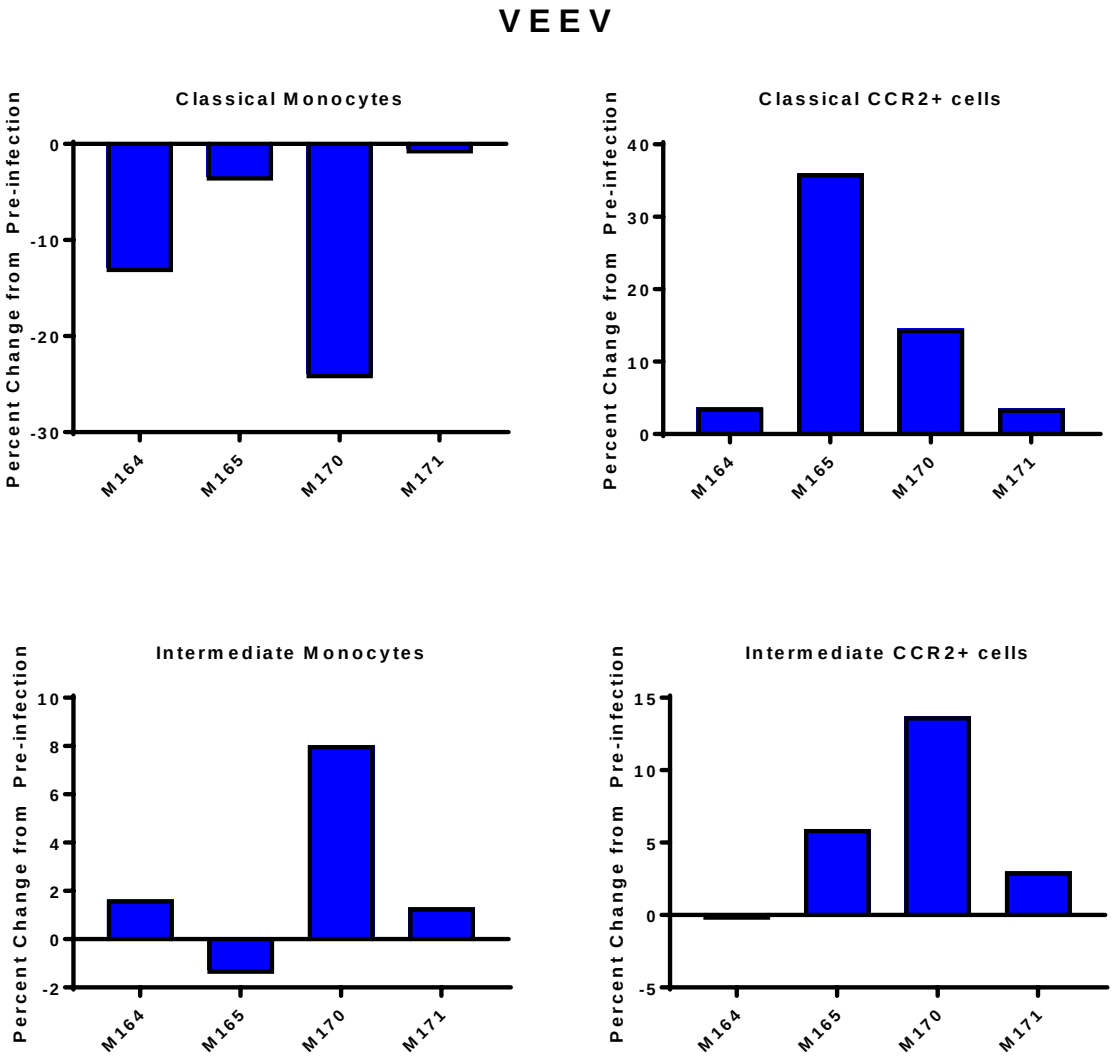

Figure 8. Change in Peripheral Immune Populations, Myeloid Lineage Continued (VEEV)

Monkeys infected with VEEV had blood collected at pre-infection and at necropsy. PBMCs were isolated from these samples and stained to identify myeloid lineage cells. Percentages were calculated using HLA-DR+, CD3-, CD20- cells as the parent population. Difference between necropsy and pre-infection shows how progression of the disease alters peripheral immune populations. No animals succumbed to infection.

Infection with VEEV presents several noticeable trends within myeloid lineage populations. There appears to be consistent increases in DN, non-classical, pDC (Figure 7), and intermediate monocyte populations, as well as a decrease in the classical monocyte population

(Figure 8). Similar to EEEV, there also appears to be an increase in the expression of CCR2 on classical and intermediate monocytes indicating immune trafficking (Figure 8).

Four animals have been challenged by aerosol route with WEEV so far in this study (M166, M167, M168, and M169). M169 reached sacrifice criteria on day 7 post infection. The other animals survived the challenge and were sacrificed at later dates (29DPI, 31DPI, and 28DPI respectively). The doses and outcomes can be found in Table 5.

Table 5. WEEV Animal, Virus, Dose, and Outcome

Animal #	Infection Date	Dose	Outcome	Necropsy
M166	1/30/17	9.88E+07	Mild Fever	29 DPI
M167	1/30/17	2.89E+08	Mild Fever	31 DPI
M168	2/13/17	2.21E+07	Mild Fever	28 DPI
M169	2/13/17	3.76E+07	Death	7 DPI

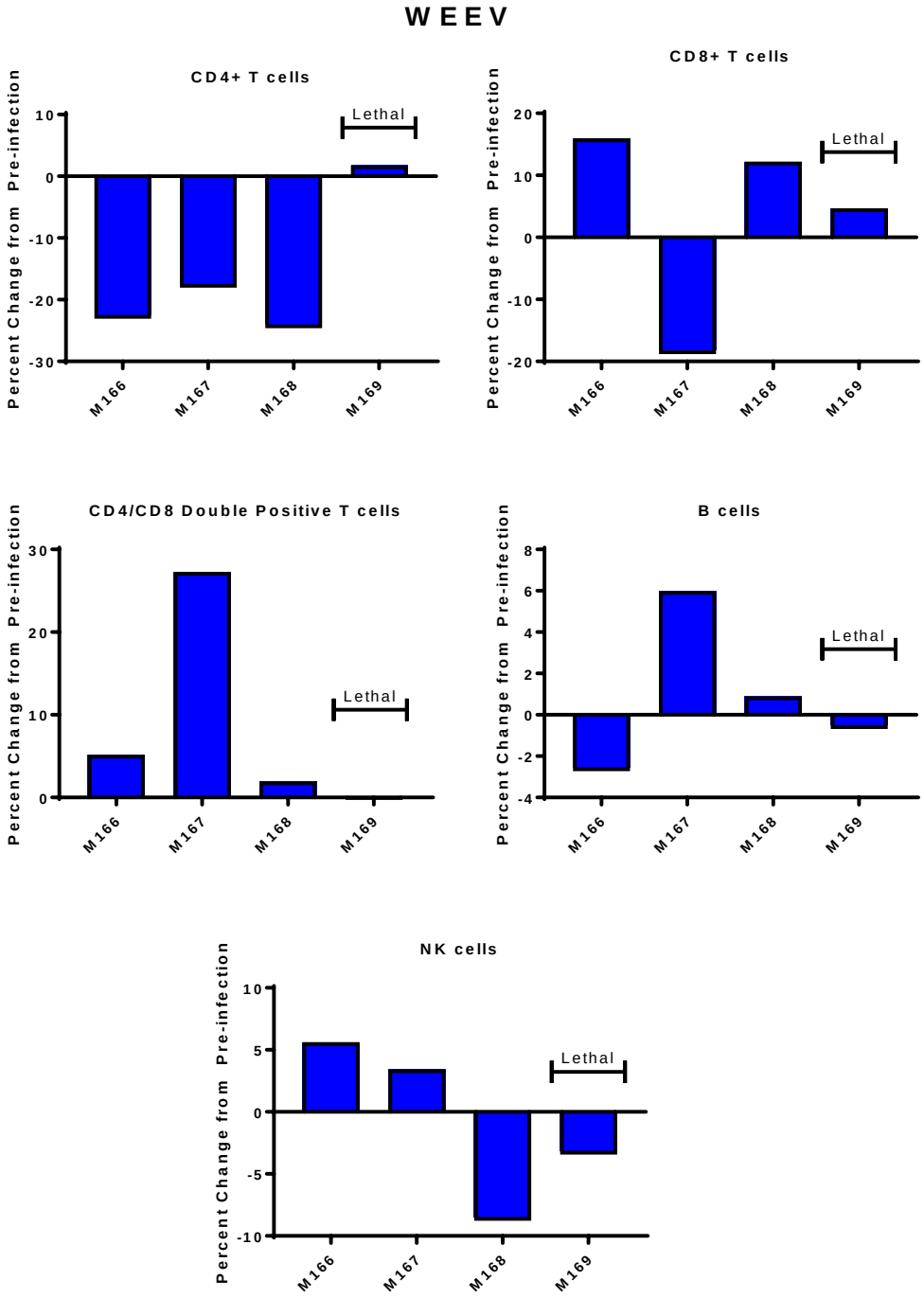

Figure 9. Change in Peripheral Immune Populations, Lymphoid Lineage (WEEV)

Monkeys infected with VEEV had blood collected at pre-infection and at necropsy. PBMCs were isolated from these samples and stained to identify lymphoid lineage cells. Percentages were calculated for B cells and NK cells using CD45 high cells minus monocyte cells (CD3-, CD20-, CD8-, HLA-DR+) as the parent population. T cell population subsets were calculated as a percentage of CD3+ cells to reduce percentage fluctuation as the result of changes in other lymphoid populations. Difference between necropsy and pre-infection shows how progression of the disease alters peripheral immune populations.

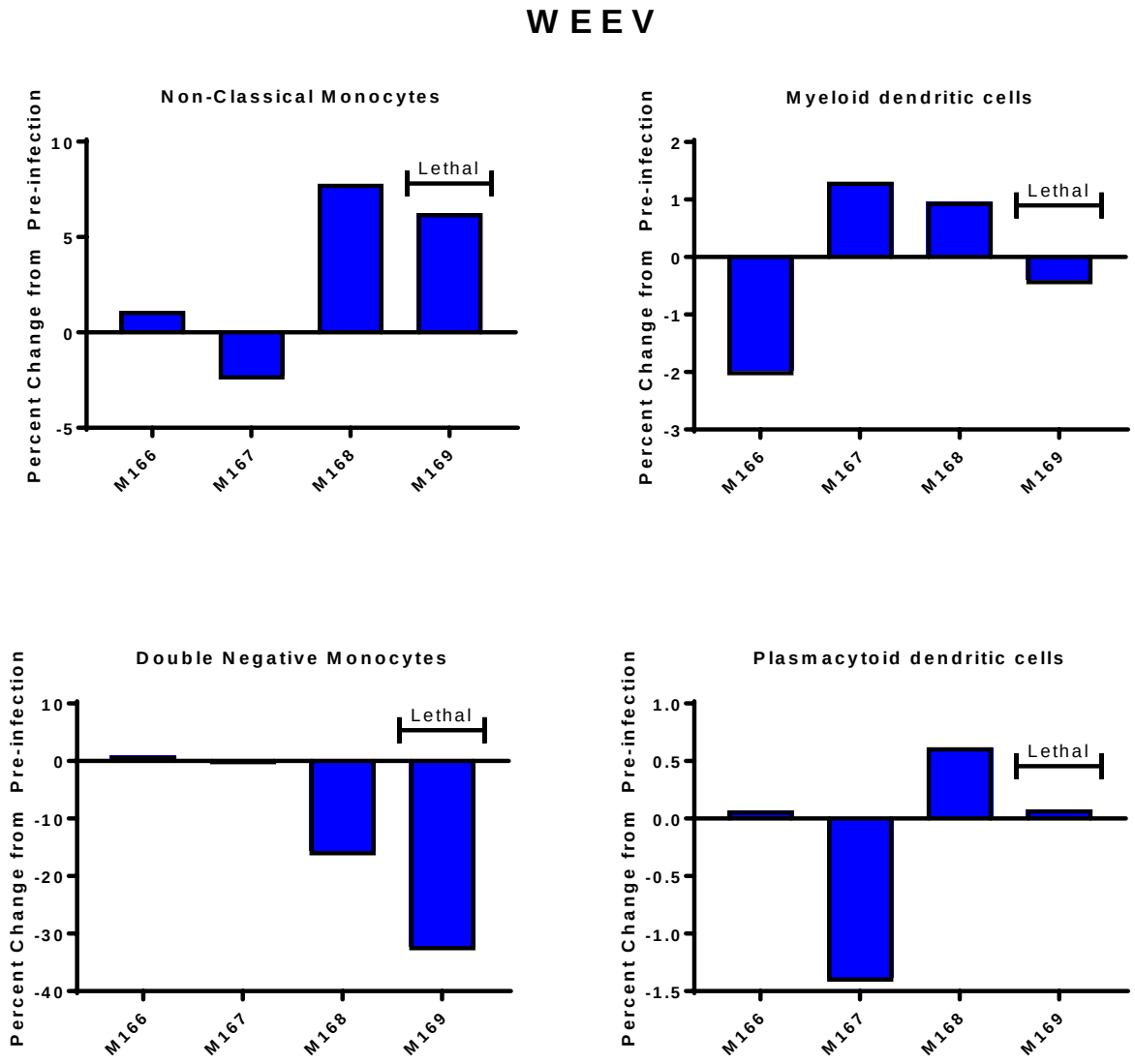

Figure 10. Change in Peripheral Immune Populations, Myeloid Lineage (WEEV)

Monkeys infected with VEEV had blood collected at pre-infection and at necropsy. PBMCs were isolated from these samples and stained to identify myeloid lineage cells. Percentages were calculated using HLA-DR+, CD3-, CD20- cells as the parent population. Difference between necropsy and pre-infection shows how progression of the disease alters peripheral immune populations.

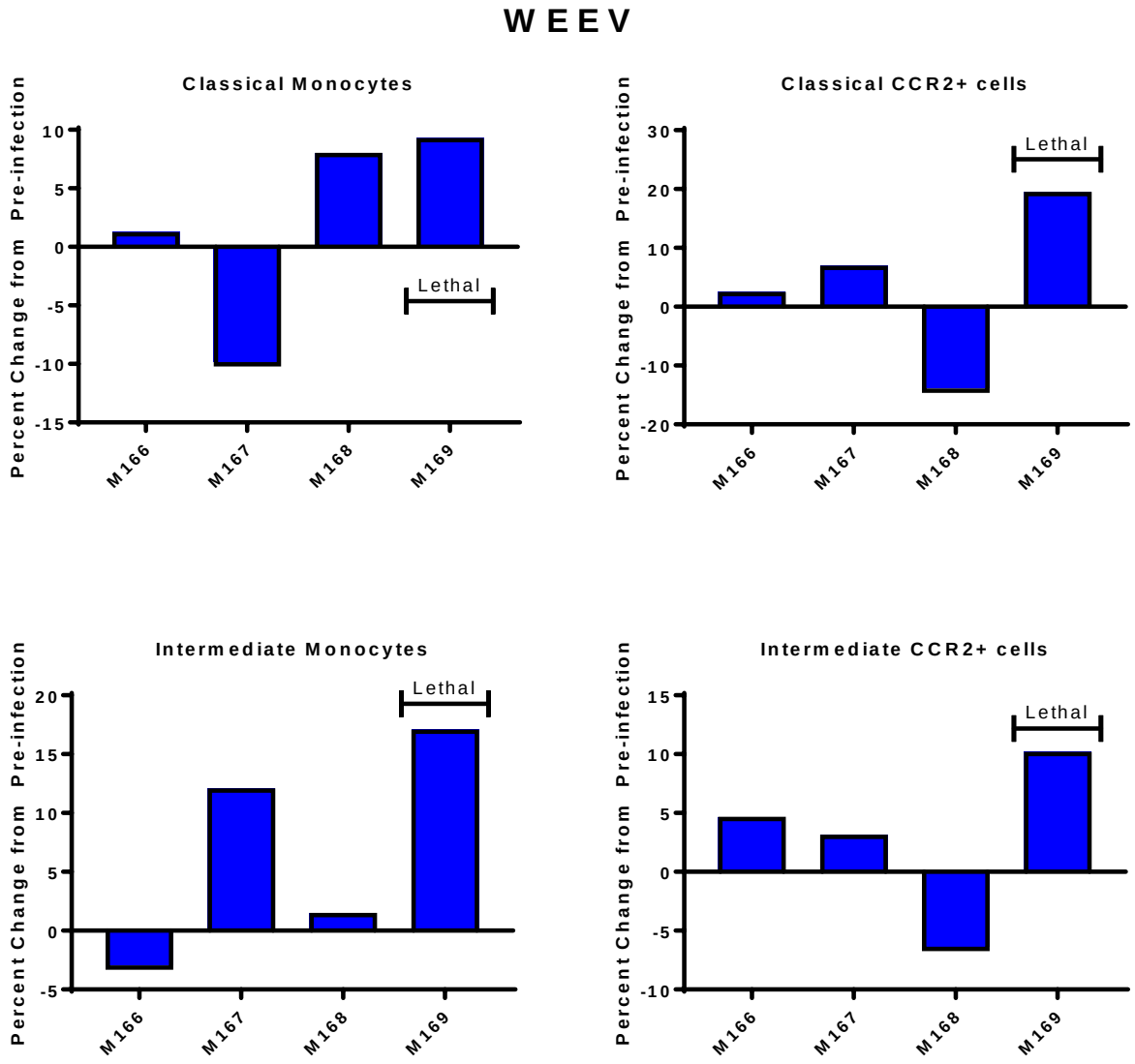

Figure 11. Change in Peripheral Immune Populations, Myeloid Lineage Continued (WEEV)

Monkeys infected with VEEV had blood collected at pre-infection and at necropsy. PBMCs were isolated from these samples and stained to identify myeloid lineage cells. Percentages were calculated using HLA-DR+, CD3-, CD20- cells as the parent population. Difference between necropsy and pre-infection shows how progression of the disease alters peripheral immune populations.

It is difficult to identify any obvious trends in the lymphoid or myeloid lineage populations in convalescent or lethally infected animals. As is consistent from myeloid lineage data from EEEV and VEEV, increases in intermediate monocyte population as well as CCR2

positive classical and intermediate populations may be a trend in WEEV infection (Figure 11). Again the bracketing to identify lethally infected animals is for visual purposes only, and does not represent any statistical comparison.

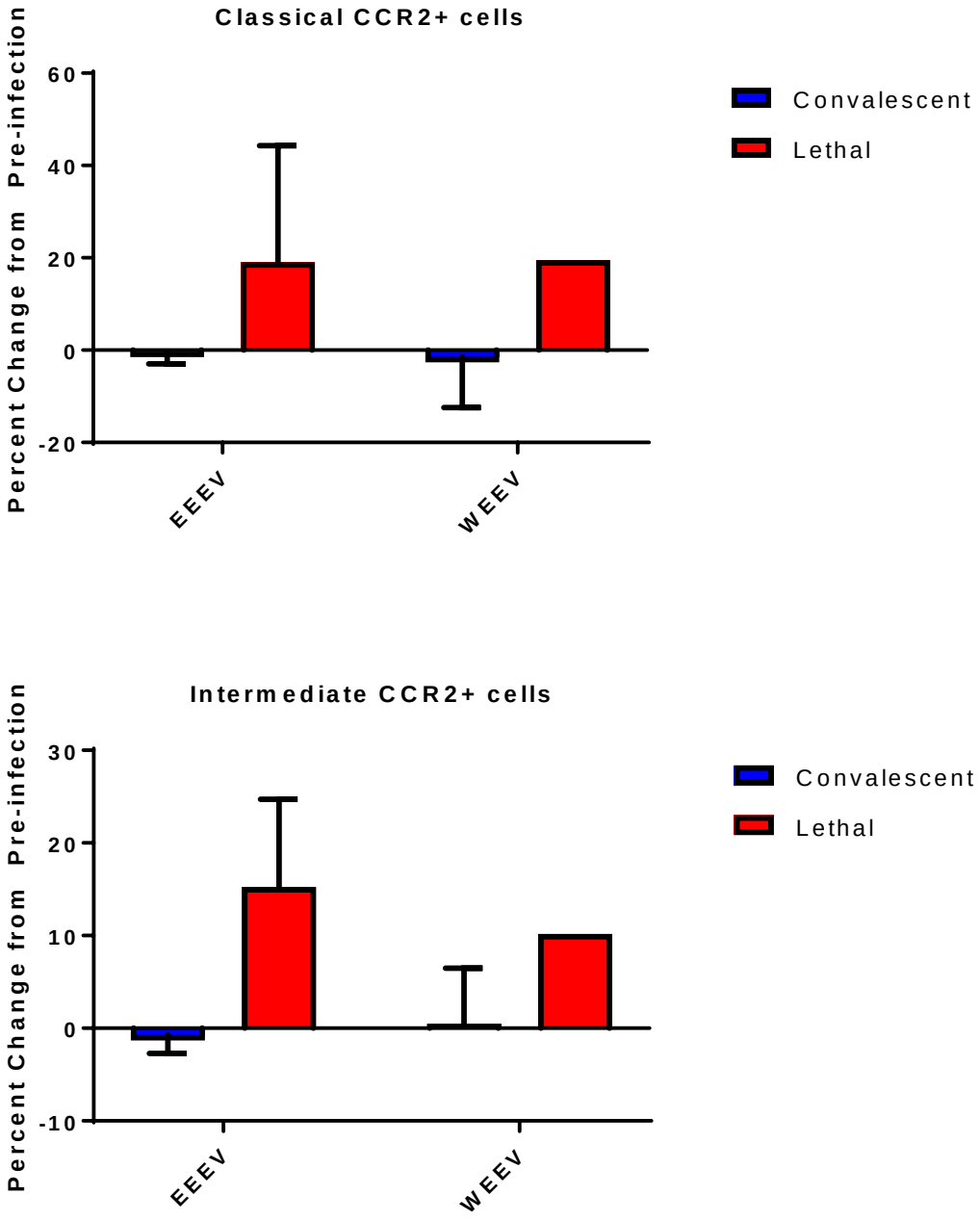

Figure 12. Difference in Brain Homing Monocyte Populations Between EEEV and WEEV

Monkeys infected with EEEV and WEEV had blood collected at pre-infection and at necropsy. PBMCs were isolated from these samples and stained to identify myeloid lineage cells. Percentages were calculated using HLA-DR+, CD3-, CD20- cells as the parent population. Difference between necropsy and pre-infection for CCR2+ classical and intermediate monocytes indicates a trend of active homing and migration of these cell types toward infected tissue.

While not statistically comparable, and in lieu of uninfected controls, animals lethally infected with EEEV and WEEV exhibit similar trends in terms of CCR2 driven classical and intermediate monocyte trafficking (Figure 12). It is more than likely that convalescent animals exhibit similar trends during peak infection, but the degree and timing of CCR2 upregulation may be a quantifiable marker of disease progression or severity once longitudinal samples are collected.

CBC analysis was done on pre-infection and necropsy blood samples using an Abaxis Vetscan HM2, and a Vetscan VS2 blood chemistry machine was used to analyze blood chemistry markers for each animal at each time point.

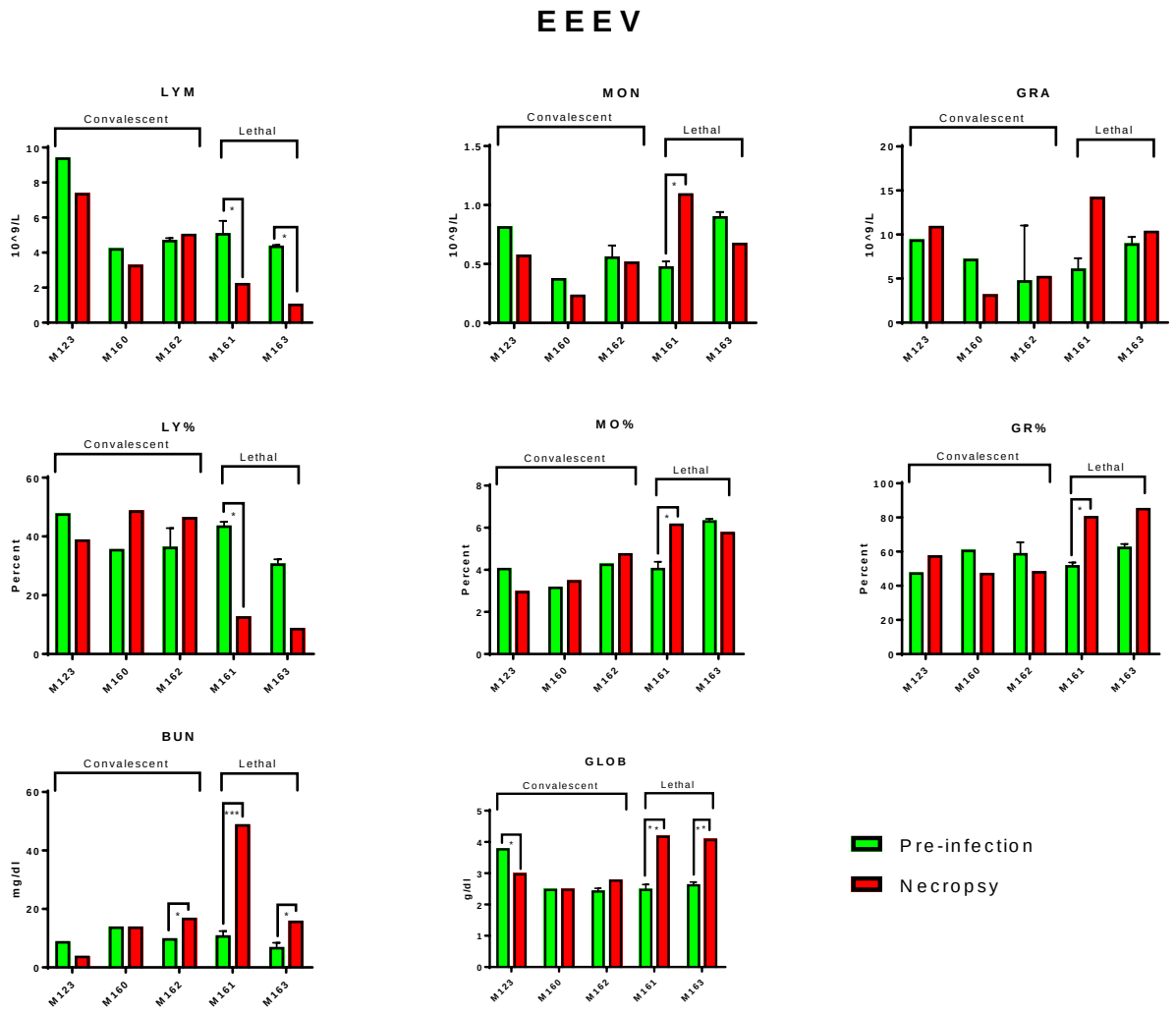

Figure 13. CBC and Significant Blood Chemistry (EEEV)

Blood test results for animals challenged with EEEV by aerosol delivery route. Samples tested pre-infection and at necropsy. Parameters of interest include lymphocytes (LYM), monocytes (MON), granulocytes (GRA), blood urea nitrogen (BUN), and globulin (GLOB). LYM, MON, and GRA shown as absolute count and as percentages. Pre-infection samples from multiple blood draws was compared to necropsy samples using a student t-test (*$p < 0.05$; **$p<.01$; ***$p<0.001$).

As expected by previous work from Reed and colleagues, monkeys lethally challenged by aerosolized EEEV exhibited lymphopenia, and granulocytosis (52). Other significant shifts as a result of lethal infection included blood urea nitrogen and globulin (Figure 13). Blood urea nitrogen is typically filtered out of the blood by the kidneys as a means to remove nitrogen from

the body. As such, it is a measure of kidney functionality and increased levels of BUN can indicate heart failure, dehydration, or kidney damage. Typically, when kidney function is impaired BUN elevation coincides with the elevation of creatinine levels in the blood. Creatinine is the product of metabolic breakdown of creatine phosphate, an energy storage molecule found in muscle tissue. As shown in figure 14, although lethally infected animals did experience an elevation in creatinine blood levels it was not statistically significant. Globulin is a collective population of proteins found in the blood that help facilitate transport of proteins across lipid barriers, clotting, and general circulation health. High globulin levels is again an indication of dehydration, but can also be elevated during inflammation, viral infection, and kidney disease to name a few. Because of differences in necropsy time points between convalescent and lethally infected animals no statistical comparisons were made between these groups. Bracketing of animals serves only to visually identify the two groups.

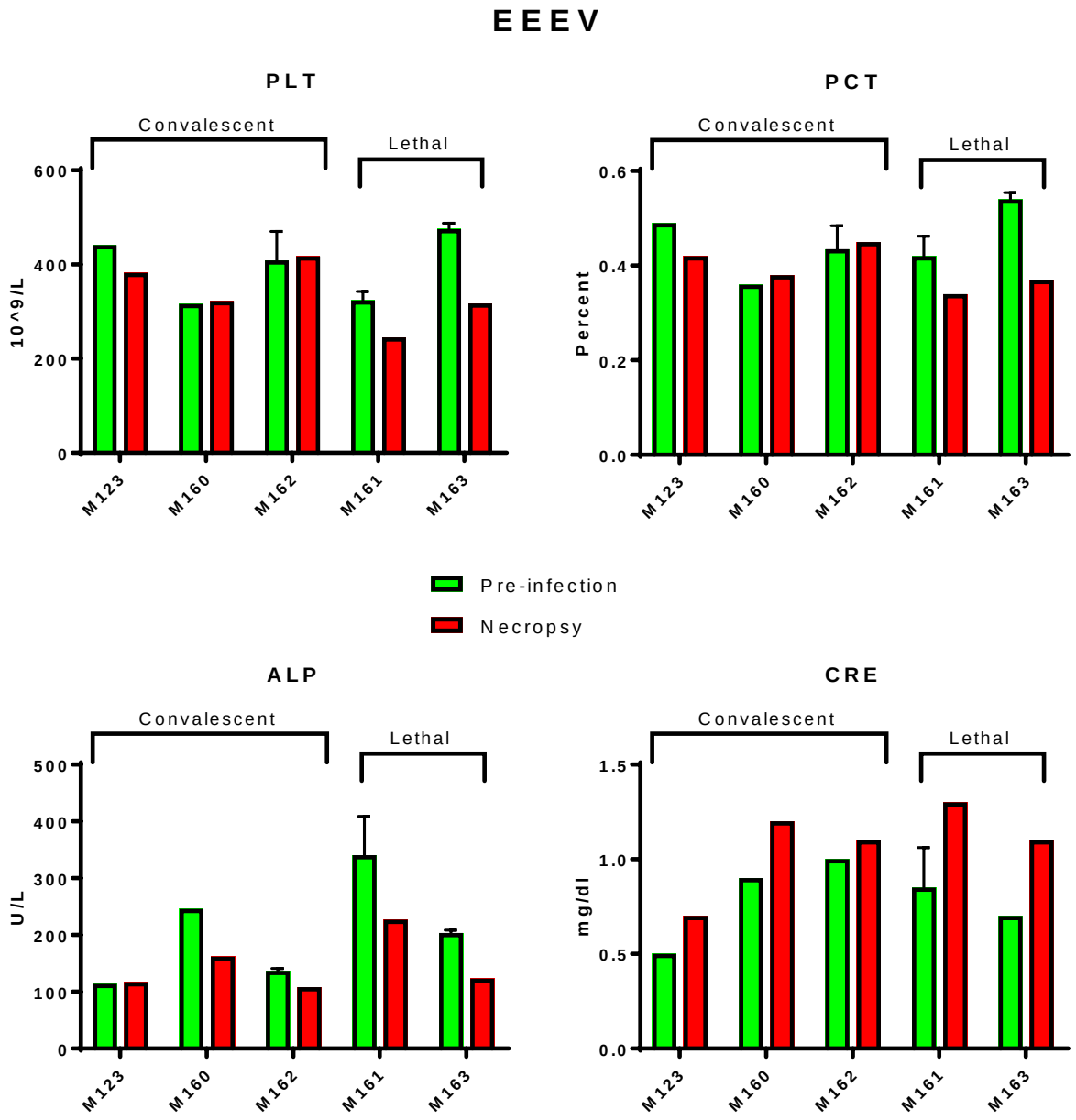

Figure 14. CBC and Blood Chemistry Trends (EEEV)

Blood test results for animals challenged with EEEV by aerosol delivery route. Samples tested pre-infection and at necropsy. Parameters of interest include platelet count (PLT), procalcitonin (PCT), alkaline phosphatase level (ALP), and creatinine (CRE). Pre-infection samples from multiple blood draws was compared to necropsy samples using a student t-test.

A general trend can be observed for animals lethally infected with EEEV suggesting thrombocytopenia and a decrease in procalcitonin levels. Thrombocytopenia could be indicative over activation of clotting factors resulting in a decrease of available platelets in the blood. It is unclear why a reduction in procalcitonin levels may occur during lethal infection since issues like sepsis and pro-inflammation are typically associated with elevation of procalcitonin. Alkaline phosphatase (ALP) is tested to determine liver function. Elevated ALP levels can indicate liver damage or dysfunction. In this case, a reduction in ALP activity may indicate malnutrition. As mentioned above, creatinine is another indication of kidney function and minor elevations can indicate dehydration. Collectively, the blood chemistry data suggests a common trend of dehydration and malnutrition in lethally infected animals. Late stage pathology of EEEV is characterized by increasingly severe neurological symptoms and as a result, we saw a substantial decrease in food and water intake in these animals. The loss of appetite and reduced water intake could explain the trends we see in the blood chemistry data.

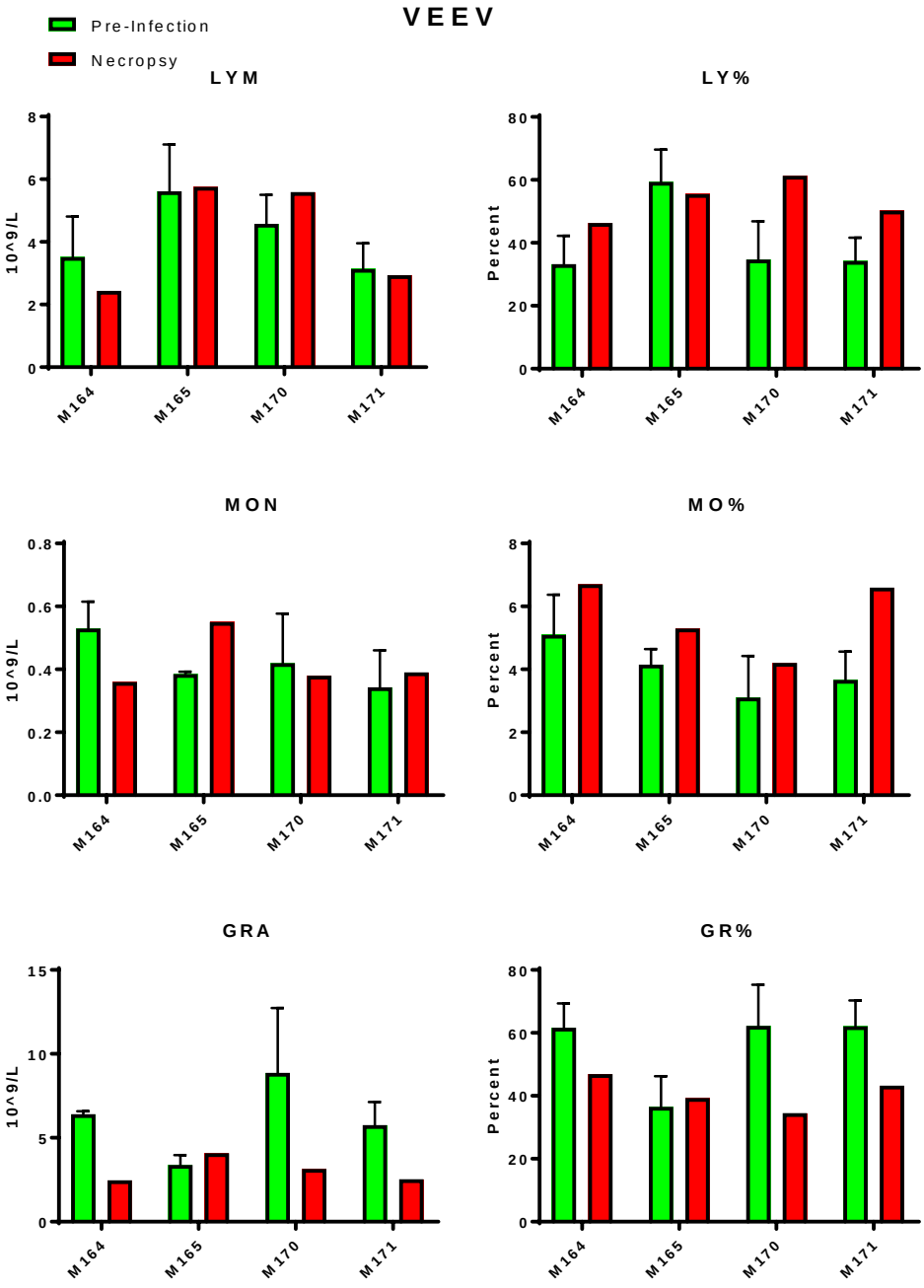

Figure 15. CBC and Blood Chemistry Trends (VEEV)

Blood test results for animals challenged with EEEV by aerosol delivery route. Samples tested pre-infection and at necropsy. Parameters of interest include lymphocytes (LYM), monocytes (MON), granulocytes (GRA). LYM, MON, and GRA shown as absolute count and as percentages. Pre-infection samples from multiple blood draws was compared to necropsy samples using a student t-test.

No statistically significant changes in CBC occurred in animals challenged with VEEV by aerosol route (Figure 15). As was noted in the VEEV flow data analysis, without lethal challenge for comparison it is difficult to identify important variations in immune response. Earlier time points may better elucidate unique changes during disease course. The blood chemistry parameters were also unremarkable. A student t-test was run on all CBC and blood chemistry parameters to confirm non-significance.

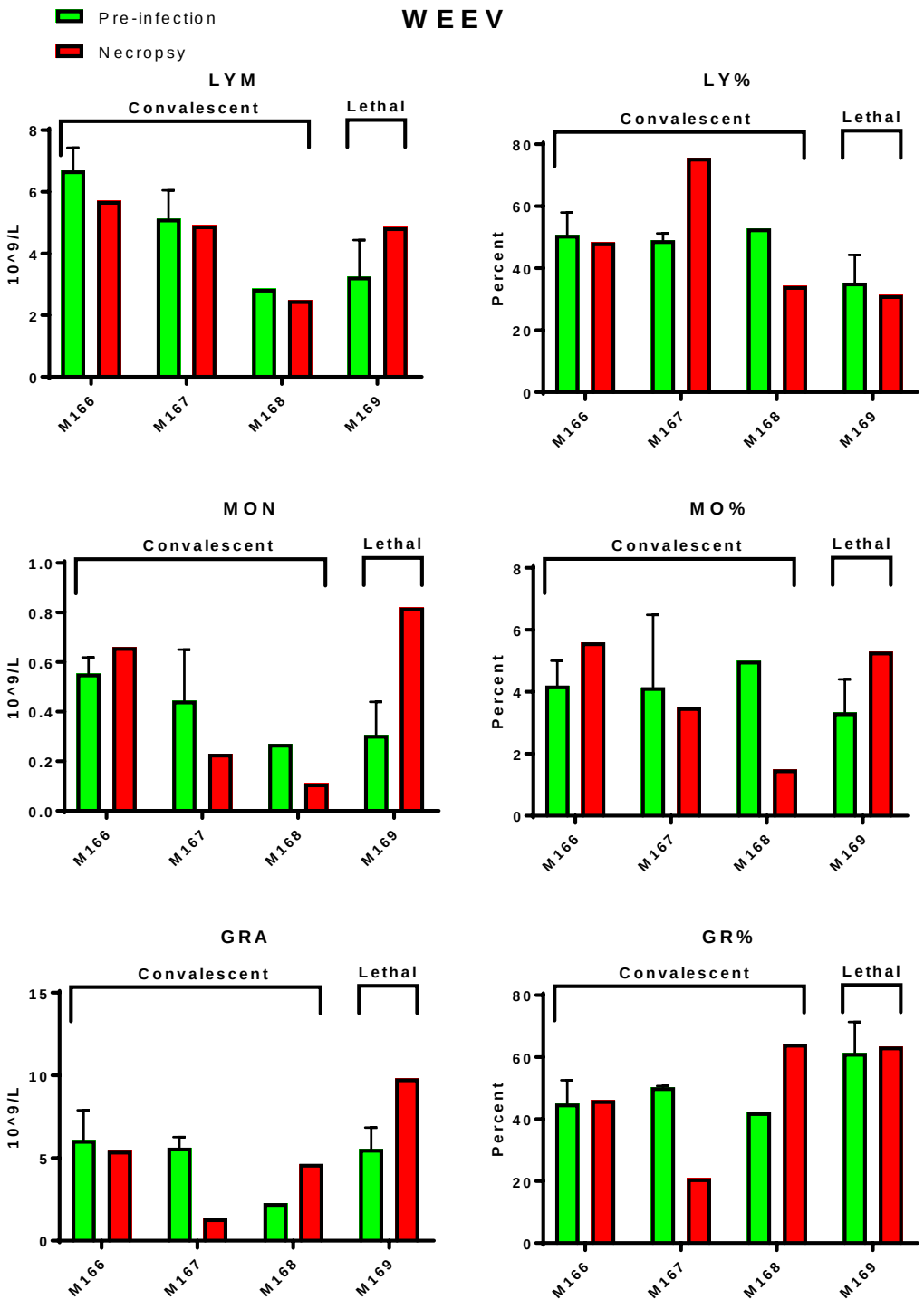

Figure 16. CBC and Blood Chemistry Trends (WEEV)

Blood test results for animals challenged with EEEV by aerosol delivery route. Samples tested pre-infection and at necropsy. Parameters of interest include lymphocytes (LYM), monocytes (MON), granulocytes (GRA). LYM, MON, and GRA shown as absolute count and as percentages. Pre-infection samples from multiple blood draws was compared to necropsy samples using a student t-test.

No statistically significant shifts in peripheral immune populations occurred in WEEV infected animals (Figure 16). More animals and earlier time points may help identify significant shifts in peripheral immune populations and blood chemistry parameters. Bracketing of convalescent and lethally infected animals is for visual identification purposes only, and does not represent a statistical comparison.

4.2 AIM 2: IDENTIFY PERIPHERAL INFLAMMATORY BIOMARKERS ASSOCIATED WITH LETHAL VS SUBLETHAL DISEASE IN THE PLASMA AND CSF, AND CORRELATE THESE FINDINGS WITH BRAIN TISSUE

During viral encephalitis, death can occur when swelling from inflammation places sufficient pressure on the brainstem to cease function. Alternatively, viral replication can cause cytotoxicity and destruction of neuronal cells, damaging the integrity of the CNS. The brainstem regulates vital bodily functions such as respiration and heart rate. It is unclear if the degree of inflammation is the result of viral replication or overactive immune responses, but the severity of inflammation may be an indicator of disease progression or potential lethality. In addition, the types of inflammatory cytokine upregulation may also provide information regarding the route of neuroinvasion. Certain inflammatory cytokines are known to cause vascular leakage and to weaken the blood brain barrier (53, 54). By looking at the inflammatory environment in brain tissue and correlating that with cerebrospinal fluid (CSF) and plasma, we may be able to identify trends in accessible peripheral samples that indicate progression in the CNS.

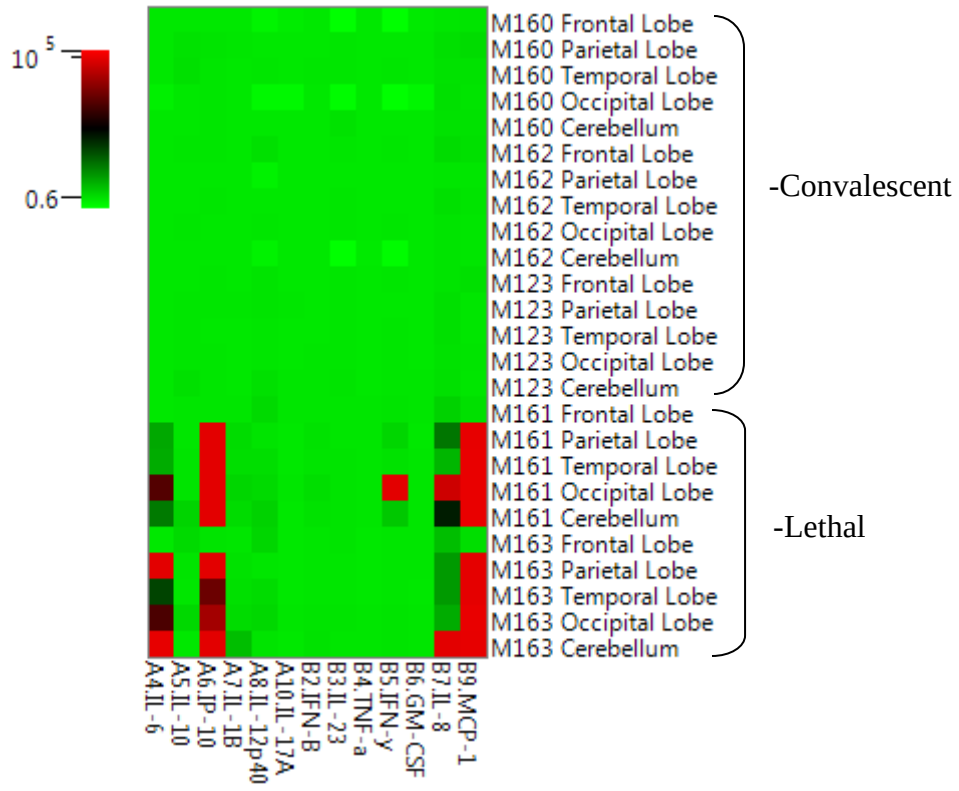

Figure 17. Biolegend LEGENDplex by Brain Region (EEEV)

Brain sections (0.3g in weight) collected from monkeys during necropsy were placed in 1.5mL of 1% DPBS with penicillin/streptomycin and stored at -80˚C. Samples were later thawed and homogenized using a handheld electric homogenizer. The homogenate was spun at 2500rpm, for 10 minutes at room temperature. Clarified supernatant was collected and used for LEGENDplex assay. Samples from survivors were analyzed without dilution, while samples from lethally infected animals were diluted 1:2 in LEGENDplex assay buffer. Scale is in pg/mL. Monkeys M161 and M163 were lethally challenged with EEEV; M123, M160, and M162 were survivors.

Samples taken from lethally infected monkeys show high levels of expression of inflammatory cytokines IL-6, IP-10, IL-8, and MCP-1 (Figure 17). MCP-1 or Monocyte Chemoattractant Protein 1 is also referred to as CCL2, the ligand responsible for attracting monocytes, memory T cells, and dendritic cells via the surface receptor CCR2. The increase of CCL2 (MCP-1) in the brains of lethally infected monkeys suggests that the observed increase of CCR2 on monocyte populations is leading to CNS homing and migration. It is impossible to rule out the possible of homing to other tissues as well without broad tissue cytokine expression analysis, but leukocyte neuroinvasion is a significant factor in the development of viral

encephalitis. MCP-1 is also known to affect the integrity of the blood brain barrier (55). Depending on the timing of upregulation of this cytokine during disease pathogenesis, this could be a major factor in viral entry into the CNS or cause permeabilization after viral entry. IP-10, also known as CXCL10, is another chemoattractant for monocytes/macrophages, T cells, NK cells, and dendritic cells, which interacts with CXCR3. Monocytes, fibroblasts, and endothelial cells typically secrete IP-10 as a response to IFN-γ.

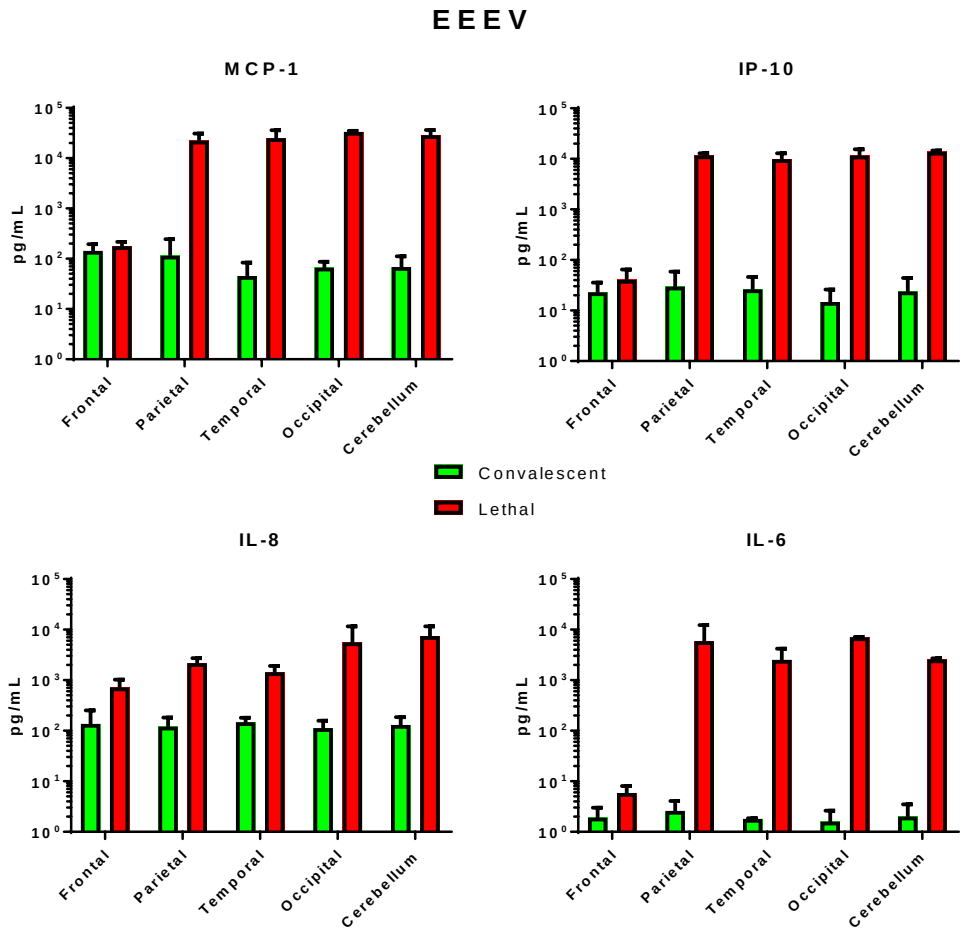

Figure 18. Inflammatory Cytokine Expression in CNS (EEEV)

Brain sections (0.3g in weight) collected from monkeys during necropsy were placed in 1.5mL of 1% DPBS with penicillin/streptomycin and stored at -80˚C. Samples were later thawed and homogenized using a handheld electric homogenizer. The homogenate was spun at 2500rpm, for 10 minutes at room temperature. Clarified supernatant was collected and used for LEGENDplex assay. Samples from survivors were analyzed without dilution, while samples from lethally infected animals were diluted 1:2 in LEGENDplex assay buffer. Data from survivors and lethally infected animals was averaged. No statistical comparison were made between these groups.

Averages from convalescent samples and lethal samples are graphically shown to demonstrate the magnitude of expression at both time points (Figure 18). No uninfected control data is available at this stage of the project because of the destructive nature of sample collection for this analysis. Later stages of the project will include uninfected animals for statistical comparison. It is likely that expression levels for most of these cytokines is substantially lower in uninfected animals. Studies looking at the CNS or CSF for uninfected animals show levels of inflammatory expression ranging from 10^2 to 10^0 depending on the cytokine in question (56). Future uninfected samples will be analyzed to verify these findings and as statistical comparison

In addition to MCP-1 and IP-10 elevated expression, IL-6 and IL-8 are also elevated in lethally infected animals (Figures 17,18). IL-6 is responsible for stimulating the synthesis of acute phase proteins (APP), a part of the innate immune system. APPs are typically released by the liver in response to inflammatory cytokines and promote innate immune pathways such as complement fixation, C-reactive protein activation, and clotting factor activation to name a few. IL-8 is another cytokine that activates APPs during the febrile response and promotes inflammation. Both IL-6 and IL-8 can be secreted by macrophages as a result of pattern recognition receptor activation. In addition to innate modulation, IL-8 also plays a role in the chemotaxis of granulocytes, specifically neutrophils as well as their degranulation. Interestingly, the frontal lobe of both lethally infected animals shows little to no inflammatory cytokine expression.

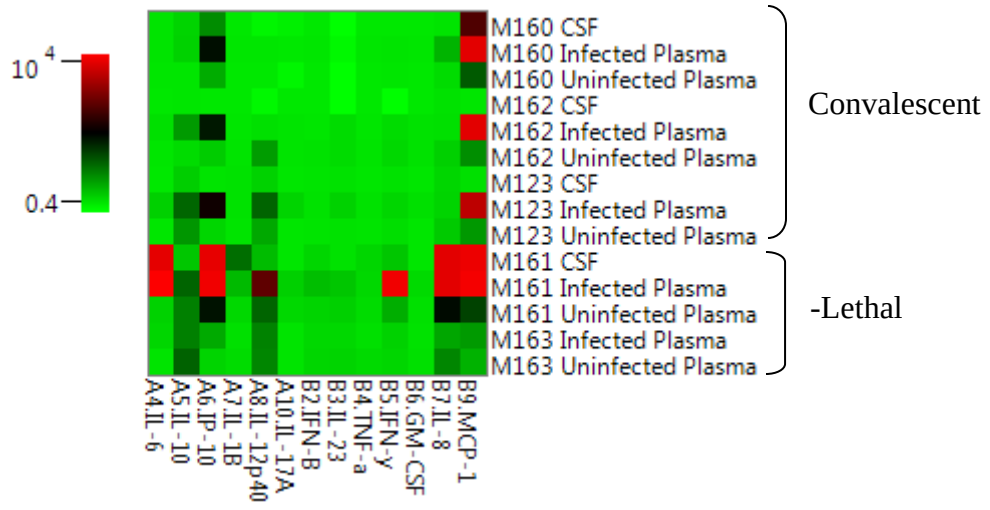

Figure 19. Biolegend LEGENDplex of Cerebrospinal Fluid and Plasma (EEEV)

CSF taken at necropsy and plasma taken either pre-infection or at necropsy were analyzed by LEGENDplex for expression levels of inflammatory cytokines. All plasma samples diluted 1:4 in LEGENDplex assay buffer. Lethally infected animal CSF samples were diluted 1:2 in LEGENDplex assay buffer; survivor CSF was run undiluted. Concentration shown in pg/mL.

The CSF taken from lethally infected animal M161 closely resembled inflammatory cytokine expression in the brain, indicating the CSF may be a useful means for identifying viral encephalitis progression. Unfortunately, CSF was not successfully extracted from M163 during necropsy, making comparative analysis impossible. In addition, although M161 plasma taken at necropsy also indicates a strong parallel between peripheral cytokines and CNS inflammation, plasma from M163 at necropsy does not. Another important note is that, although we consider the survivors convalescent at this point, there is an obvious increase in inflammatory cytokines in plasma taken from necropsy compared to pre-infection. Although the difference is not statistically significant because of variations between animals, it indicates that nearly a month later, and with no infectious virus detected by plaque assay, these animals are not fully recovered.

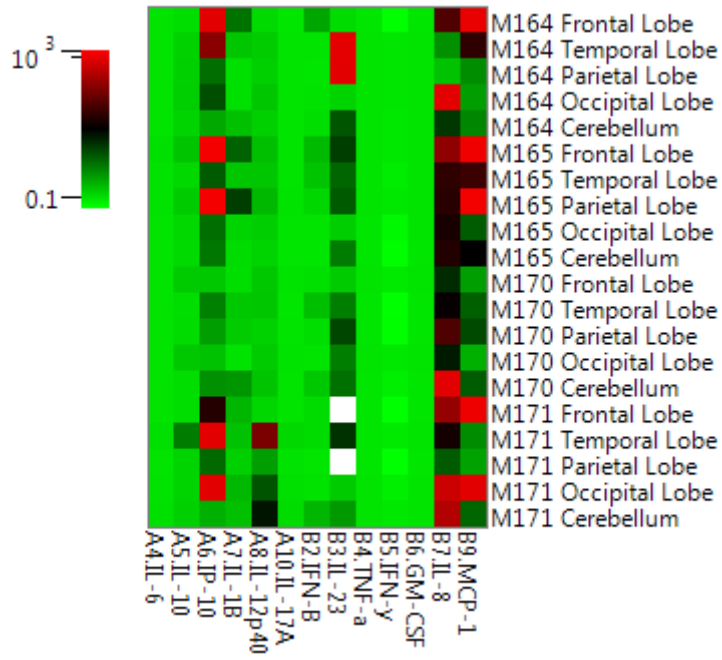

Figure 20. Biolegend LEGENDplex by Brain Region (VEEV)

Brain sections (0.3g in weight) collected from monkeys during necropsy were placed in 1.5mL of 1% DPBS with penicillin/streptomycin and stored at -80˚C. Samples were later thawed and homogenized using a handheld electric homogenizer. The homogenate was spun at 2500rpm, for 10 minutes at room temperature. Clarified supernatant was collected and used for LEGENDplex assay. All samples run without dilution. Scale is in pg/mL. No animals succumbed to VEEV infection, all samples taken at convalescence. IL-23 beads had reduced numbers or were absent in a number of samples, represented here by the two blank squares for M171 samples.

Although no VEEV animals ultimately succumbed to infection, a substantial amount of inflammation remains present in the brain. In EEEV and WEEV the distribution of inflammatory markers was fairly uniform throughout the brain, but in the case of VEEV there appears to be localized distribution (Figure 20). Although this could be the result of unequal recovery times for different brain regions, it could also be a unique difference resulting from the method in neuroinvasion. Although the exact method of neural invasion by EEEV and WEEV is unknown, one theory is that passive diffusion after permeabilization of the blood brain barrier is the cause, explaining a uniform distribution of inflammation. VEEV on the other hand, is theorized to gain viral entry through infiltrating dendritic cells from peripheral tissues (33). In addition, VEEV monkeys exhibit no upregulation of IL-6. This could support the theory that IL-6 levels recover

quickly as animals become convalescent, or it could indicate that VEEV infected animals do not experience an elevation in IL-6 expression as is seen with EEEV and WEEV.

The upregulation of IL-23 and IL-12p40 in some animals represents a pattern not seen in EEEV and WEEV infected animals. IL-23 is typically associated with activation of a Th17 response thereby promoting inflammation. IL-23 is a heterodimer (IL-23p19 and IL-12p40) that binds to the IL-23 receptor, another heterodimer composed of IL-12R β1 and IL-23R. The changes in IL-23 expression shown here are still under review considering a possible problem with the LEGENDplex kit used for the assay.. IL-12p40, as a subunit of IL-23. It is secreted by activated macrophages and serves as an inducer for a Th1 response. IL-12p40 is important in sustaining effector T cell numbers in order to establish a memory population, but overexpression in the brain has been implicated with neurodegenerative disorders such as multiple sclerosis.

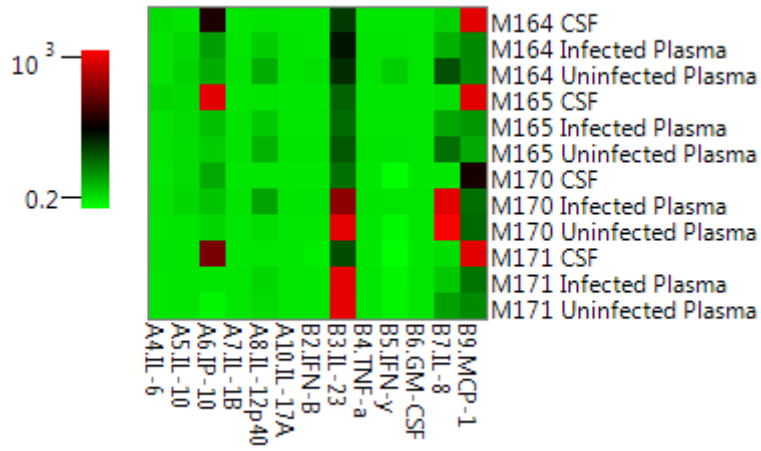

Figure 21. Biolegend LEGENDplex of Cerebrospinal Fluid and Plasma (VEEV)

CSF taken at necropsy and plasma taken either pre-infection or at necropsy were analyzed by LEGENDplex for expression levels of inflammatory cytokines. All plasma samples diluted 1:4 in LEGENDplex assay buffer; CSF was run undiluted. Concentration shown in pg/mL.

Inflammatory markers in the CSF demonstrate close parallels with CNS inflammation. Plasma taken at necropsy represents a poor surrogate of CNS inflammation, as is the case with EEEV and WEEV samples. Although it has some similarities to CNS inflammation, it is

inconsistent with the inflammation seen in the brain regions and CSF. There is also inconsistency of upregulation of inflammation markers in the plasma between animals.

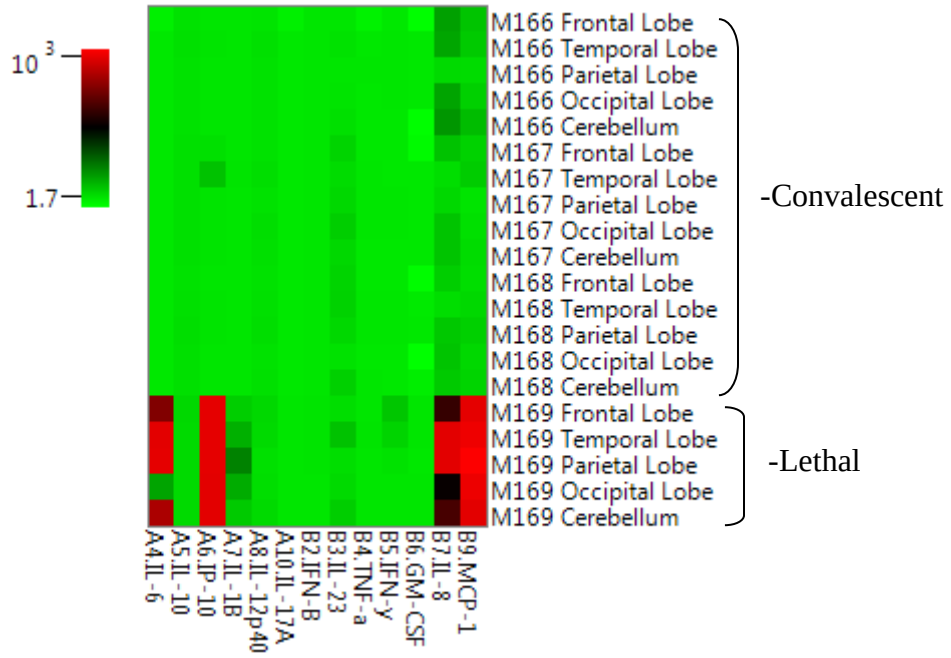

Figure 22. Biolegend LEGENDplex by Brain Region (WEEV)

Brain sections (0.3g in weight) collected from monkeys during necropsy were placed in 1.5mL of 1% DPBS with penicillin/streptomycin and stored at -80˚C. Samples were later thawed and homogenized using a handheld electric homogenizer. The homogenate was spun at 2500rpm, for 10 minutes at room temperature. Clarified supernatant was collected and used for LEGENDplex assay. Samples from survivors were analyzed without dilution, while samples from lethally infected animals were diluted 1:2 in LEGENDplex assay buffer. Scale is in pg/mL. Monkey M169 was lethally challenged with WEEV; M166, M167, and M168 were survivors.

Inflammatory activation in animals lethally infected with WEEV demonstrates an almost identical pattern to that observed for lethal EEEV infection. Once again MCP-1, IL-8, IL-6, and IP-10 are elevated throughout the brain of the lethally challenged animal. The striking similarity is not entirely unexpected when considering WEEV's genetic origin as a recombinant of Sindbis-like virus and EEEV.

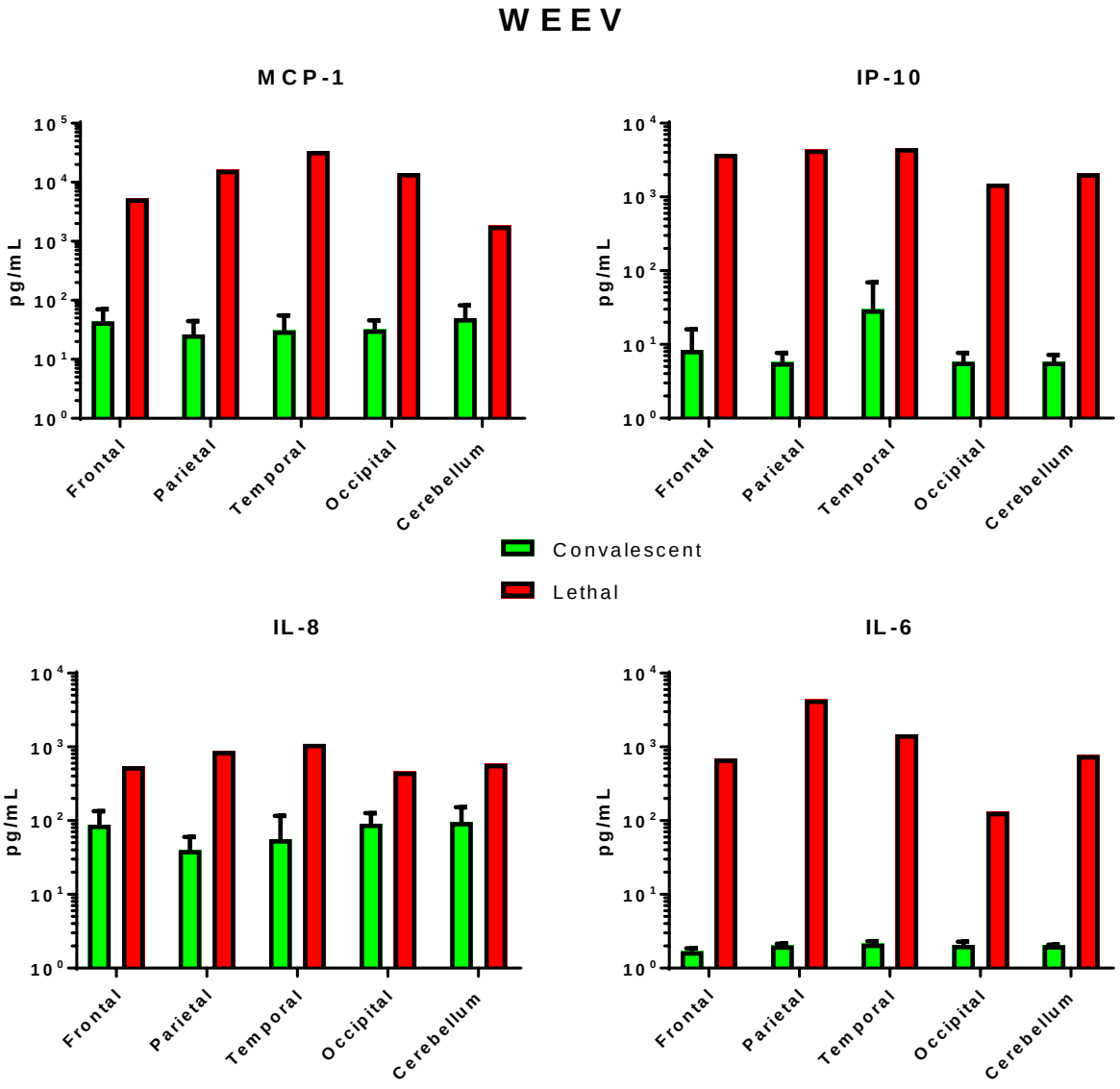

Figure 23. Inflammatory Cytokine Expression in CNS (WEEV)

Brain sections (0.3g in weight) collected from monkeys during necropsy were placed in 1.5mL of 1% DPBS with penicillin/streptomycin and stored at -80˚C. Samples were later thawed and homogenized using a handheld electric homogenizer. The homogenate was spun at 2500rpm, for 10 minutes at room temperature. Clarified supernatant was collected and used for LEGENDplex assay. Samples from survivors were analyzed without dilution, while samples from lethally infected animals were diluted 1:2 in LEGENDplex assay buffer. Data from survivors was averaged. No statistical comparison was made between these samples due to differences in time points.

As was the case with EEEV, we see a similar elevation in MCP-1, IP-10, IL-8, and IL-6 (Figure 23). In general, although the pattern of cytokine expression appears similar, the animals

lethally infected with EEEV exhibit higher concentrations of these four inflammatory cytokines when directly compared to WEEV (4-5 fold difference), which could explain the difference in mortality rate between the two viruses although more animals are needed to for a sufficient statistical comparison.

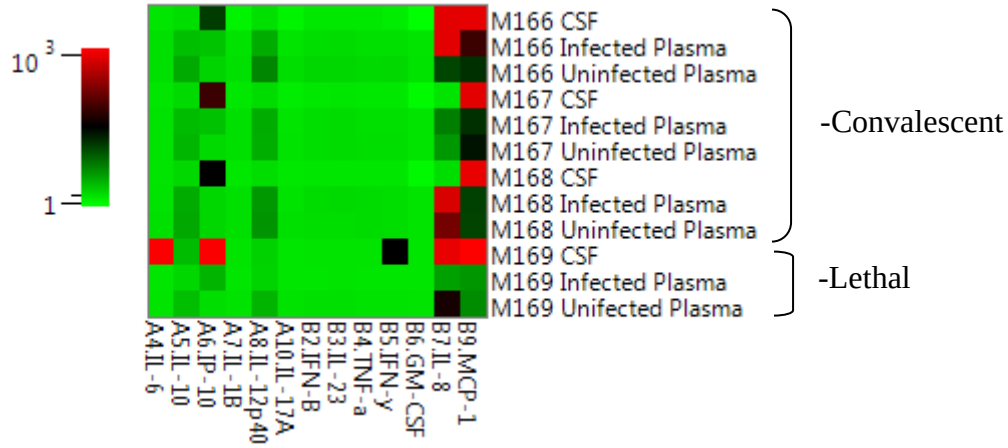

Figure 24. Biolegend LEGENDplex of Cerebrospinal Fluid and Plasma (WEEV)

CSF taken at necropsy and plasma, taken either pre-infection or at necropsy, were analyzed by LEGENDplex for expression levels of inflammatory cytokines. All plasma samples diluted 1:4 in LEGENDplex assay buffer. Lethally infected animal (M169) CSF sample was diluted 1:2 in LEGENDplex assay buffer; convalescent CSF was run undiluted. Concentration shown in pg/mL.

The concentration of inflammatory cytokines in the CSF in a similar pattern to the brain of the lethally challenged animal again demonstrates that continuing inflammatory dysregulation is occurring even after virus is no longer detectable by plaque assay (Figure 24). It is unclear if the residual inflammatory response is the result of latent virus in immune privileged tissues, or simply a gradual return to homeostasis. Similar to EEEV and VEEV, we see that plasma taken at necropsy is an inconsistent surrogate for CNS inflammation. Although it shows upregulation of similar inflammatory cytokines in some animals, it is not consistent with the CSF or brain regions. It remains to be seen if this holds true at earlier time points, or if the expression of inflammatory markers in the plasma occurs in a delayed fashion relative to the CNS. IL-6 is only

elevated in the CSF of the lethally infected animal. The other inflammatory markers associated with the CNS are minimally elevated in the CSF of one or more survivors, but IL-6 is only present in the animal with active and lethal infection. This could imply that IL-6 represents a marker of severity of CNS inflammation as compared to the other elevated markers. If true, reduction in IL-6 expression during disease course could also be an indication of survival and recovery, even if other inflammatory markers remain elevated.

5.0 DISCUSSION

New World alphaviruses are important arboviral pathogens with the potential for further geographical spread and severe impact to human health. Epizootic outbreaks cause substantial harm to equine populations and have the potential to cause human infection (4). Human disease can range in severity from minor febrile illness to severe encephalitis and death, and survivors can develop long-term neurological sequelae (1). Even in the case of VEEV, which has less than 1% mortality rate, debilitating disease has the potential to cause significant economic disruption. The USDA classifies EEEV and VEEV as Select Agents because of the severe threat they pose to human and animal health (57). In addition, NIAID classifies all three pathogens as Category B priority emerging infectious diseases (58). Both these classifications recognize the threat New World alphaviruses pose through bioterrorism or natural outbreaks. In order to address this threat, it is important to understand the pathogenesis of each virus to identify potential targets for therapeutics or vaccines.

No FDA approved vaccines or treatments currently exist for these viruses, and given their morbidity, human trials are unethical. As such, a primate model is paramount to the development and testing of novel therapeutics, utilizing the FDA animal rule. The ongoing goal of this study is to develop a non-human primate model for alphavirus infection by an aerosol route. The initial phase of this project was to observe complete disease progression, develop an ID100 for each virus, and identify potential quantifiable markers of disease severity.

It is important to note that longitudinal samples were not collected in order to observe disease progression without confounding variables. As a result, the final time points of the study are not directly comparable. Samples collected from animals at convalescent are not comparable to lethally infected samples because of differences of 2 weeks or more between time points. It is impossible to rule out the possibility that the same trends and patterns seen in lethally infected animals also occurs in convalescent animals at earlier time points. In addition, although markers identified at this stage of the study will be scrutinized later during longitudinal sample collection, it is possible that late stage disease effects on cytokines or peripheral immune population trends are entirely different at earlier stages. Although we may focus on trends in CCR2 cells, and cytokines CCL2, IP-10, IL-8, and IL-6, it will be important to continue taking a broad approach to sample collection and data analysis to avoid missing quantifiable markers not identified by this study.

One unique aspect of this study is the method by which the viral stocks were produced. As shown by Klimstra and colleagues (59, 60), alphaviruses passaged multiple times in mammalian cells significantly alters the expression of viral attachment and entry factors, specifically the E2 glycoprotein. As a result, these viruses are adapted toward growth and infection in mammalian cultures, but have less severe clinical outcomes *in vivo.* The increased binding affinity of E2 to heparan sulfate (HS) on mammalian cells can limit the degree of viral dissemination during inoculation, thereby reducing viremia and reducing the neuroinvasiveness in some species of alphavirus. In order to avoid this complication, the Klimstra laboratory generated cDNA clones based on sequences acquired from human clinical isolates and modified them to better represent naturally circulating viruses. These cDNA clones were used to generate viral RNA genomes, which were then transfected into cells. Virus stock was then collected from

the supernatant of these transfected cells and passaged once using Vero E6 cells. These single passage stocks possess the HS binding characteristics of naturally circulating viruses and are therefore not attenuated like alphaviruses passaged in cell culture.

Due to limited space in the BSL-3, only 3 or four monkeys could be housed within the facility at any given time. As a result, most animals were kept at an offsite facility prior to virus challenge. When initial pre-infection blood draws were performed on these animals, blood samples had to be transported back to the containment facility before being processed. The lengthy delay between blood draw and blood processing dramatically reduced the viability of some samples for flow cytometry, and created hemolytic errors when used for CBC or blood chemistry analysis. Most of these samples were not included in the statistically analysis. Fortunately, blood samples were also collected the day of each animal's exposure after they were brought to the BSL-3 facility, but quantities of blood taken at that time varied based on the size and hydration of each animal.

Since blood PBMCs were initially isolated and freshly stained, a live/dead stain was not included in the initial flow cytometry panels. When viably frozen samples were thawed for re-staining purposes, the use of fixable live/dead stains caused significant compensation problems for several important markers. The added live/dead UV stain reduced the separation of CD16 by CD14, making the myeloid panel ineffective in identifying subsets within the monocyte population. This was due to difficulty separating the close emission spectrum of BV412 and V500 when live/dead UV stain was present. Despite ultimately removing the live/dead stain, additional efforts were taken to ensure the quality of re-stained cells. Two doublet exclusion gates were used, and none of the characteristic signs of lysed cells were present in the final stains. Because of their autofluorescence across a broad number of channels, dead cells often

cause easily identifiable diagonal populations at medium mean fluorescent intensity. By increasing the forward scatter threshold, dead cells and any platelet contamination that was not removed during PBMC isolation was excluded from analysis.

When cynomolgus macaques were infected with EEEV, it resulted in death in 2 out of 5 animals. Both lethally infected animals developed a fever roughly 72 hours after inoculation and rapidly declined on day 5 post infection. Symptoms included head pressing, rocking, glassy eyes, and reduced activity or response to stimuli. Both animals reached the humane endpoint on day 6 when they became moribund and unresponsive. The three survivors were either asymptomatic or developed mild acute febrile symptoms. The collection of neurological tissue from both survivors and lethally infected animals revealed no observable gross anatomical changes such as calcifications or necrosis during necropsy. Further more detailed histopathology analysis of these tissues is ongoing and may demonstrate characteristic encephalopathy. The cerebrospinal fluid proved somewhat more difficult to collect in some animals than others, and no CSF was successfully collected from the first animal necropsied (M163). Minor contamination of CSF with blood could potentially have affected the LEGENDplex assay results.

The results from flow staining on PBMCs indicate a rise in CD4 T cells, but a reduction of CD8 and CD4/CD8 double positive cells. It is unclear if this shift in the population is the result of CD8 cells trafficking to the CNS, or if the virus is causing targeted cell death within these populations. The role of CD4/CD8 double positive T cells is unclear in this context. While some papers have demonstrated a strong anti-viral function, others have identified cytokine production and helper T cell like functions more commonly associated with CD4 cells (61, 62). The phenotype of these cells could be elucidated further using live cell sorting and identifying intracellular cytokine production, but at this stage it remains ambiguous. Another population that

appears altered from pre-infection to necropsy for lethally challenged animals is the NK cell population. NK cells are a first line of defense and also produce a number of immune modulatory cytokines that are important for inflammation and viral clearance. The loss of these cells could indicate migration elsewhere, or depletion as a result of activation, nevertheless it will be important to identify trends in NK cells in earlier time points as potential indications of disease progression or severity. The next step in these studies will be to compare flow cytometry results in PBMC isolated from whole blood to immune cells isolated from the brain to see if the changes seen in the peripheral immune populations coincide with changes in the CNS. A preliminary look into neural immune cell results suggests a large number of lymphocytes and, to a smaller extent, myeloid cells. Unpublished data by JA from our lab, suggests that, of the macrophages that are present in CNS tissue, a majority of the classical and intermediate cell populations are CCR2+ and CD163+, indicating that they are perivascular in origin and not resident microglial cells (63).

The large increases in CCR2+ classical and intermediate monocyte subpopulations demonstrate a potential drive towards neurotrafficking. It is unclear if these cells are infected and serving as Trojan horses assisting neuroinvasion, or if they are responding to pro-inflammatory signals produced after viral invasion into the CNS. Research in mice suggests that EEEV is incapable of replicating in myeloid cell lineages, although this requires verification in NHP (15). The significance of CCR2 and CCL2 (MCP-1) in chronic inflammation and autoimmune disorders of the CNS are already well characterized with experimental autoimmune encephalomyelitis (64). Whether this is virus driven or inflammation driven, it offers a potential target for therapeutic intervention. Targeting CCL2 function is already a technique being investigated to prevent metastasis of cancer to bone marrow (65). Aside from homing and

migration to infected tissue, CCL2 is also expressed by osteoblasts to recruit osteoclasts for bone synthesis. This is especially interesting in the case of EEEV because research in mice suggests the viruses initial site of replication is in cells of mesenchymal origin, specifically fibroblasts which are in close relation to osteoblasts (15). While this was not a focus at this stage of the project, it is possible that the same chemoattractant may play a role in neuroinvasion as well as the initial site of replication.

It is important to note that flow cytometry analysis of pre-infections samples demonstrated a surprising amount of variability between animals and between pre-infection collections for animals that had more than one pre-infection blood draw. Future analysis may require more pre-infection collection and analysis to strengthen statistical comparisons.

The inflammatory cytokine expression in animals lethally infected with EEEV showed elevation of MCP-1 (CCL2), IP-10, IL-6, and IL-8. The increased expression of MCP-1 could be a possible target for therapeutic agents. IP-10 has many similar functions to MCP-1 in promoting migration of immune cells into the CNS. IP-10 interacts with the CXCR3 receptor found on activated T cells and NK cells. Given the elevated levels of IP-10 it is worthwhile to explore CXCR3 expression on these cell types as a potential factor in neuroinvasion by T cells and NK cells. IL-8 is primarily thought to recruit neutrophils, and, in some forms of encephalitis, neutrophils are seen in the CSF and regions of the brain. Initial work in the CNS suggests lymphocytes and monocytes are the primary infiltrating immune cells during equine encephalitis, but the role of neutrophils may need to be examined further if IL-8 is playing a significant role. IL-6 is produced by a number of immune cells including T cells and macrophages and promotes the acute phase response (66-68). It is a major activator of the febrile response and is present at considerably high levels in lethally infected animals. The most interesting trend observed for IL-

6 expression in the CNS during lethal infection is the relative absence of IL-6 in convalescent animals. Although they have lower expression of MCP-1, IP-10, and IL-8 compared to levels in lethally infected animals, they still are present at concentrations ranging from several hundred to a thousand pg/mL in animals nearly 30 days after infection. IL-6 on the other hand is expressed at or below 10pg/mL in every brain region of each convalescent animal. Although it is not clear how quickly IL-6 levels return to normal, it could be an important marker for determining survival. IL-6 has already been shown to have protective roles in other encephalitis diseases such as HSV (69).

An important aspect of the project was finding biological surrogates for inflammation in the brain. To this end, CSF seemed to mirror CNS inflammation and demonstrated similar patterns of upregulation in lethally infected animals and in convalescence. Unfortunately, plasma was an inconsistent surrogate with some samples showing no inflammation similar to brain regions, or showing altered patterns of upregulation. While CSF collection is moderately invasive and difficult, it still demonstrates an accessible and reliable indicator of disease severity and progression. When longitudinal samples are collected at later stages of this project, plasma may be more indicative of disease progression at earlier time points. All three viruses cause viremia shortly after infection. While each virus progresses to this viremia at different rates, the peak viremia of each virus may stimulate peripheral inflammation that can serve as quantifiable markers of disease severity. As shown in mice (15), VEEV viremia is detectable 6 hrs p.i. and peaks at 18 hrs p.i. On the other hand, viremia is not detectable in EEEV until 24 hrs p.i. and peaks at 48 hrs p.i. These could represent valuable time points for longitudinal samples in identifying quantifiable indicators of disease progression.

Some important concerns regarding the LEGENDplex assay should be mentioned. The first assay, which was performed on samples from EEEV infected monkeys, had problems regarding clumping when run on the FACSAria flow cytometer. While samples were spun down after initial homogenization, they were not spun down again immediately prior to dilution for the LEGENDplex assay. As a result, the samples had to be filtered again before being run on the flow cytometer. This could explain the slightly larger standard deviation as each sample is run in duplicate. This problem was fixed in later plates. Another problem that was encountered was the absence or substantial reduction in the number of IL-23 specific beads in the assay performed on samples from VEEV infected animals. Given the questionable results for IL-23, it will be disregarded in these data sets.

For the myeloid stain, it was difficult identifying trends in myeloid dendritic cells and Plasmacytoid dendritic cells because of the relative size of these populations. Although a very small portion of the monocyte population, they represent unique effector cells. The stain confirms our ability to isolate these cells for future live cell isolation or intracellular cytokine staining to assess their phenotype and activation in infected animals. Intracellular staining or live cell sorting could also be important for lymphocyte populations such as CD4 cells to determine their phenotype.

In conclusion, analysis by flow cytometry of animals infected with EEEV, VEEV, and WEEV suggests shifts in T cell populations (CD4, CD8), NK cells, and the classical and intermediate subsets of the broader monocyte population. These changes in classical and intermediate cell populations coincide with a substantial increase in the expression of CCR2, a receptor responsible for homing and migration to infected tissues. Furthermore, there is an increase in expression of MCP-1 (CCL-2) in the brains of lethally infected animals, suggesting a

potential for neuroinvasion by monocytes and lymphocytes. Brains of lethally infected animals also presented with elevation of IP-10 (CXCL-10), IL-8, and IL-6, with IL-6 elevation being unique to lethally challenged animals. These inflammatory markers could represent targets of therapeutic treatment, or markers of disease severity and progression. By observing these same chemokines/cytokines at earlier time points, we may be able to identify onset of viral encephalitis, and likelihood of eventual disease mortality. These cytokines also provide potential investigative routes for future studies. Part of the larger project included continual telemetry data of temperature and ECG. If these same markers have altered expression in the periphery, they could be responsible for certain cardiac abnormalities. IP-10 (CXCL-10) for example, is a marker of acute heart injury and infarct, and MCP-1 (CCL-2) is expressed by a number of peripheral cell types such as osteoblasts and fibroblasts, which means leukocyte infiltration into cardiac or pulmonary tissue may occur as well. In addition, given our knowledge of alphavirus promiscuity of cell tropism (especially VEEV), it is impossible to rule out migration of immune cells to a variety of tissues. VEEV also commonly causes a systemic pathology compared to EEEV and WEEV, which are primarily encephalitis (70). While this study has focused on chemokine expression in the brain and suggestive migration to the CNS, it is important to note the potential for viral infection in peripheral tissues and subsequent leukocyte homing systemically. Finally, flow analysis of CCR2 expression on classical and intermediate monocytes from whole blood, combined with LEGENDplex analysis of CSF, may be examples of moderately accessible peripheral samples with diagnostic potential for alphavirus induced encephalitis. Taken at longitudinal time points these combined data sets could help identify important clinical windows during alphavirus infection.

BIBLIOGRAPHY

1. **Ryman KD, Klimstra WB.** 2008. Host responses to alphavirus infection. Immunol Rev **225:**27-45.
2. **Leitenberg M, Zilinskas RA, Kuhn JH.** 2012. The Soviet biological weapons program : a history. Harvard University Press, Cambridge, Massachusetts.
3. **Go YY, Balasuriya UB, Lee CK.** 2014. Zoonotic encephalitides caused by arboviruses: transmission and epidemiology of alphaviruses and flaviviruses. Clin Exp Vaccine Res **3:**58-77.
4. **Zacks MA, Paessler S.** 2010. Encephalitic alphaviruses. Vet Microbiol **140:**281-286.
5. **Health TCfFSP.** 2015. Eastern, Western, and Venezuelan Equine Encephalomyelitis. Accessed
6. **Kondig JP, Turell MJ, Lee JS, O'Guinn ML, Wasieloski LP, Jr.** 2007. Genetic analysis of South American eastern equine encephalomyelitis viruses isolated from mosquitoes collected in the Amazon Basin region of Peru. Am J Trop Med Hyg **76:**408-416.
7. **Armstrong PM, Andreadis TG.** 2013. Eastern equine encephalitis virus--old enemy, new threat. N Engl J Med **368:**1670-1673.
8. **Feemster RF.** 1938. Outbreak of Encephalitis in Man Due to the Eastern Virus of Equine Encephalomyelitis. Am J Public Health Nations Health **28:**1403-1410.
9. **Przelomski MM, O'Rourke E, Grady GF, Berardi VP, Markley HG.** 1988. Eastern equine encephalitis in Massachusetts: a report of 16 cases, 1970-1984. Neurology **38:**736-739.
10. **Scott TW, Weaver SC.** 1989. Eastern equine encephalomyelitis virus: epidemiology and evolution of mosquito transmission. Adv Virus Res **37:**277-328.
11. **Weaver SC, Scott TW, Rico-Hesse R.** 1991. Molecular evolution of eastern equine encephalomyelitis virus in North America. Virology **182:**774-784.
12. **Arrigo NC, Adams AP, Weaver SC.** 2010. Evolutionary patterns of eastern equine encephalitis virus in North versus South America suggest ecological differences and taxonomic revision. J Virol **84:**1014-1025.
13. **Aguilar PV, Robich RM, Turell MJ, O'Guinn ML, Klein TA, Huaman A, Guevara C, Rios Z, Tesh RB, Watts DM, Olson J, Weaver SC.** 2007. Endemic eastern equine encephalitis in the Amazon region of Peru. Am J Trop Med Hyg **76:**293-298.
14. **Deresiewicz RL, Thaler SJ, Hsu L, Zamani AA.** 1997. Clinical and neuroradiographic manifestations of eastern equine encephalitis. N Engl J Med **336:**1867-1874.
15. **Gardner CL, Burke CW, Tesfay MZ, Glass PJ, Klimstra WB, Ryman KD.** 2008. Eastern and Venezuelan equine encephalitis viruses differ in their ability to infect

dendritic cells and macrophages: impact of altered cell tropism on pathogenesis. J Virol **82:**10634-10646.

16. **Vogel P, Kell WM, Fritz DL, Parker MD, Schoepp RJ.** 2005. Early events in the pathogenesis of eastern equine encephalitis virus in mice. Am J Pathol **166:**159-171.
17. **Griffin DE, Levine B, Tyor WR, Tucker PC, Hardwick JM.** 1994. Age-dependent susceptibility to fatal encephalitis: alphavirus infection of neurons. Arch Virol Suppl **9:**31-39.
18. **Levine B, Goldman JE, Jiang HH, Griffin DE, Hardwick JM.** 1996. Bc1-2 protects mice against fatal alphavirus encephalitis. Proc Natl Acad Sci U S A **93:**4810-4815.
19. **Vernon PS, Griffin DE.** 2005. Characterization of an in vitro model of alphavirus infection of immature and mature neurons. J Virol **79:**3438-3447.
20. **Robert W Derlet M, Iris Reyes M, Sarah M perman M, MS.** 2016. Venezuelan Equine Encephalitis. Medscape Journal of Medicine.
21. **Koprowski H, Cox HR.** 1947. Human laboratory infection with Venezuelan equine encephalomyelitis virus; report of four cases. N Engl J Med **236:**647-654.
22. **Reed DS, Lind CM, Sullivan LJ, Pratt WD, Parker MD.** 2004. Aerosol infection of cynomolgus macaques with enzootic strains of venezuelan equine encephalitis viruses. J Infect Dis **189:**1013-1017.
23. **Aguilar PV, Estrada-Franco JG, Navarro-Lopez R, Ferro C, Haddow AD, Weaver SC.** 2011. Endemic Venezuelan equine encephalitis in the Americas: hidden under the dengue umbrella. Future Virol **6:**721-740.
24. **Carrara AS, Coffey LL, Aguilar PV, Moncayo AC, Da Rosa AP, Nunes MR, Tesh RB, Weaver SC.** 2007. Venezuelan equine encephalitis virus infection of cotton rats. Emerg Infect Dis **13:**1158-1165.
25. **Brault AC, Powers AM, Holmes EC, Woelk CH, Weaver SC.** 2002. Positively charged amino acid substitutions in the e2 envelope glycoprotein are associated with the emergence of venezuelan equine encephalitis virus. J Virol **76:**1718-1730.
26. **Lord RD.** 1974. History and geographic distribution of Venezuelan equine encephalitis. Bull Pan Am Health Organ **8:**100-110.
27. **Estrada-Franco JG, Navarro-Lopez R, Freier JE, Cordova D, Clements T, Moncayo A, Kang W, Gomez-Hernandez C, Rodriguez-Dominguez G, Ludwig GV, Weaver SC.** 2004. Venezuelan equine encephalitis virus, southern Mexico. Emerg Infect Dis **10:**2113-2121.
28. **Weaver SC, Salas R, Rico-Hesse R, Ludwig GV, Oberste MS, Boshell J, Tesh RB.** 1996. Re-emergence of epidemic Venezuelan equine encephalomyelitis in South America. VEE Study Group. Lancet **348:**436-440.
29. **Rico-Hesse R, Weaver SC, de Siger J, Medina G, Salas RA.** 1995. Emergence of a new epidemic/epizootic Venezuelan equine encephalitis virus in South America. Proc Natl Acad Sci U S A **92:**5278-5281.
30. **Weaver SC, Anishchenko M, Bowen R, Brault AC, Estrada-Franco JG, Fernandez Z, Greene I, Ortiz D, Paessler S, Powers AM.** 2004. Genetic determinants of Venezuelan equine encephalitis emergence. Arch Virol Suppl**:**43-64.
31. **Steele KE, Twenhafel NA.** 2010. REVIEW PAPER: pathology of animal models of alphavirus encephalitis. Vet Pathol **47:**790-805.
32. **MacDonald GH, Johnston RE.** 2000. Role of dendritic cell targeting in Venezuelan equine encephalitis virus pathogenesis. J Virol **74:**914-922.

33. **Charles PC, Walters E, Margolis F, Johnston RE.** 1995. Mechanism of neuroinvasion of Venezuelan equine encephalitis virus in the mouse. Virology **208:**662-671.
34. **Watts DM, Callahan J, Rossi C, Oberste MS, Roehrig JT, Wooster MT, Smith JF, Cropp CB, Gentrau EM, Karabatsos N, Gubler D, Hayes CG.** 1998. Venezuelan equine encephalitis febrile cases among humans in the Peruvian Amazon River region. Am J Trop Med Hyg **58:**35-40.
35. **Fulton JS.** 1938. A Report of Two Outbreaks of Equine Encephalomyelitis in Saskatchewan. Can J Comp Med **2:**39-46.
36. **Barnett HC.** 1956. The transmission of Western equine encephalitis virus by the mosquito Culex tarsalis Coq. Am J Trop Med Hyg **5:**86-98.
37. **Barker CM, Johnson WO, Eldridge BF, Park BK, Melton F, Reisen WK.** 2010. Temporal connections between Culex tarsalis abundance and transmission of western equine encephalomyelitis virus in California. Am J Trop Med Hyg **82:**1185-1193.
38. **Bergren NA, Auguste AJ, Forrester NL, Negi SS, Braun WA, Weaver SC.** 2014. Western equine encephalitis virus: evolutionary analysis of a declining alphavirus based on complete genome sequences. J Virol **88:**9260-9267.
39. **CDC.** 2010. Western equine encephalitis virus neuroinvasive disease cases reported by state, 1964-2010. Accessed
40. **Forrester NL, Kenney JL, Deardorff E, Wang E, Weaver SC.** 2008. Western Equine Encephalitis submergence: lack of evidence for a decline in virus virulence. Virology **380:**170-172.
41. **Hahn CS, Lustig S, Strauss EG, Strauss JH.** 1988. Western equine encephalitis virus is a recombinant virus. Proc Natl Acad Sci U S A **85:**5997-6001.
42. **Zlotnik I, Peacock S, Grant DP, Batter-Hatton D.** 1972. The pathogenesis of western equine encephalitis virus (W.E.E.) in adult hamsters with special reference to the long and short term effects on the C.N.S. of the attenuated clone 15 variant. Br J Exp Pathol **53:**59-77.
43. **Morse SS.** 2005. Equine Encephalitis, Venezuelen, and Related Alphaviruses, p *In* (ed), Encyclopedia of Bioterrorism Defense, ed vol John Wiley & Sons, Inc.,
44. **Gould EA, Higgs S.** 2009. Impact of climate change and other factors on emerging arbovirus diseases. Trans R Soc Trop Med Hyg **103:**109-121.
45. **David R. Franz DVM, PH.D.; Cheryl D. Parrott; Ernest T. Takafuji, M.D., M.P.H.** 1997. The U.S. Biological Warfare and Biological Defense Programs. Textbook of Military Medicine: Medical Aspects of Chemical and Biological Warfare., Washington, DC: US Deptartment of the Army, Surgeon General, and the Borden Institute.
46. **Riedel S.** 2004. Biological warfare and bioterrorism: a historical review. Proc (Bayl Univ Med Cent) **17:**400-406.
47. **Reichert E, Clase A, Bacetty A, Larsen J.** 2009. Alphavirus antiviral drug development: scientific gap analysis and prospective research areas. Biosecur Bioterror **7:**413-427.
48. **Davis NL, Willis LV, Smith JF, Johnston RE.** 1989. In vitro synthesis of infectious venezuelan equine encephalitis virus RNA from a cDNA clone: analysis of a viable deletion mutant. Virology **171:**189-204.
49. **Davis NL, Powell N, Greenwald GF, Willis LV, Johnson BJ, Smith JF, Johnston RE.** 1991. Attenuating mutations in the E2 glycoprotein gene of Venezuelan equine

encephalitis virus: construction of single and multiple mutants in a full-length cDNA clone. Virology **183:**20-31.

50. **FDA US.** 2015. Product Development Under the Animal Rule. Administration USDoHaHSFaD,
51. **Brooke CB, Deming DJ, Whitmore AC, White LJ, Johnston RE.** 2010. T cells facilitate recovery from Venezuelan equine encephalitis virus-induced encephalomyelitis in the absence of antibody. J Virol **84:**4556-4568.
52. **Reed DS, Lackemeyer MG, Garza NL, Norris S, Gamble S, Sullivan LJ, Lind CM, Raymond JL.** 2007. Severe encephalitis in cynomolgus macaques exposed to aerosolized Eastern equine encephalitis virus. J Infect Dis **196:**441-450.
53. **Varatharaj A, Galea I.** 2017. The blood-brain barrier in systemic inflammation. Brain Behav Immun **60:**1-12.
54. **Rochfort KD, Cummins PM.** 2015. The blood-brain barrier endothelium: a target for pro-inflammatory cytokines. Biochem Soc Trans **43:**702-706.
55. **Yao Y, Tsirka SE.** 2014. Monocyte chemoattractant protein-1 and the blood-brain barrier. Cell Mol Life Sci **71:**683-697.
56. **Tarkowski E, Rosengren L, Blomstrand C, Wikkelso C, Jensen C, Ekholm S, Tarkowski A.** 1997. Intrathecal release of pro- and anti-inflammatory cytokines during stroke. Clin Exp Immunol **110:**492-499.
57. **Federal Select Agent Program U.** 2017. Select Agents and Toxins List, *on* CDC. Accessed
58. **Diseases NIoAaI.** 2016. NIAID Emerging INfectious Diseases/Pathogens. Accessed
59. **Bernard KA, Klimstra WB, Johnston RE.** 2000. Mutations in the E2 glycoprotein of Venezuelan equine encephalitis virus confer heparan sulfate interaction, low morbidity, and rapid clearance from blood of mice. Virology **276:**93-103.
60. **Gardner CL, Choi-Nurvitadhi J, Sun C, Bayer A, Hritz J, Ryman KD, Klimstra WB.** 2013. Natural variation in the heparan sulfate binding domain of the eastern equine encephalitis virus E2 glycoprotein alters interactions with cell surfaces and virulence in mice. J Virol **87:**8582-8590.
61. **Nascimbeni M, Shin EC, Chiriboga L, Kleiner DE, Rehermann B.** 2004. Peripheral CD4(+)CD8(+) T cells are differentiated effector memory cells with antiviral functions. Blood **104:**478-486.
62. **Quandt D, Rothe K, Scholz R, Baerwald CW, Wagner U.** 2014. Peripheral CD4CD8 double positive T cells with a distinct helper cytokine profile are increased in rheumatoid arthritis. PLoS One **9:**e93293.
63. **Kim WK, Alvarez X, Fisher J, Bronfin B, Westmoreland S, McLaurin J, Williams K.** 2006. CD163 identifies perivascular macrophages in normal and viral encephalitic brains and potential precursors to perivascular macrophages in blood. Am J Pathol **168:**822-834.
64. **Kim RY, Hoffman AS, Itoh N, Ao Y, Spence R, Sofroniew MV, Voskuhl RR.** 2014. Astrocyte CCL2 sustains immune cell infiltration in chronic experimental autoimmune encephalomyelitis. J Neuroimmunol **274:**53-61.
65. **Herman JG, Stadelman HL, Roselli CE.** 2009. Curcumin blocks CCL2-induced adhesion, motility and invasion, in part, through down-regulation of CCL2 expression and proteolytic activity. Int J Oncol **34:**1319-1327.

66. **Arango Duque G, Descoteaux A.** 2014. Macrophage cytokines: involvement in immunity and infectious diseases. Front Immunol **5:**491.
67. **Scheller J, Chalaris A, Schmidt-Arras D, Rose-John S.** 2011. The pro- and anti-inflammatory properties of the cytokine interleukin-6. Biochim Biophys Acta **1813:**878-888.
68. **Trinschek B, Luessi F, Haas J, Wildemann B, Zipp F, Wiendl H, Becker C, Jonuleit H.** 2013. Kinetics of IL-6 production defines T effector cell responsiveness to regulatory T cells in multiple sclerosis. PLoS One **8:**e77634.
69. **Dvorak F, Martinez-Torres F, Sellner J, Haas J, Schellinger PD, Schwaninger M, Meyding-Lamade UK.** 2004. Experimental herpes simplex virus encephalitis: a long-term study of interleukin-6 expression in mouse brain tissue. Neurosci Lett **367:**289-292.
70. **de la Monte S, Castro F, Bonilla NJ, Gaskin de Urdaneta A, Hutchins GM.** 1985. The systemic pathology of Venezuelan equine encephalitis virus infection in humans. Am J Trop Med Hyg **34:**194-202.